UNIVERSIDAD POLITÉCNICA DE MADRID

ESCUELA TÉCNICA SUPERIOR
DE INGENIEROS DE TELECOMUNICACIÓN

MASTER OF SCIENCE IN NEUROTECHNOLOGY
MASTER´S THESIS

Design and Implementation of a Brain-Computer Interface System for Lower Limb Exoskeleton Control using Deep Learning-Based Motor Imagery Classification

Sergio Manso Coloma

2025

MASTER OF SCIENCE IN NEUROTECHNOLOGY

MASTER´S THESIS

Title: Design and Implementation of a Brain-Computer Interface System for Lower Limb Exoskeleton Control using Deep Learning-Based Motor Imagery Classification

Author: Sergio Manso Coloma

Technical Supervisor: Giorgos Kontaxakis

Academic Supervisor: Álvaro Gutiérrez Martín

Department: Tecnología Fotónica y Bioingeniería

MEMBERS OF THE EXAMINATION COMMITTEE

President:

Member:

Secretary:

Substitute:

The above-named members of the panel agree to grant the qualification of: ……

Madrid, a …… 2025

UNIVERSIDAD POLITÉCNICA DE MADRID

ESCUELA TÉCNICA SUPERIOR
DE INGENIEROS DE TELECOMUNICACIÓN

MASTER OF SCIENCE IN NEUROTECHNOLOGY
MASTER´S THESIS

Design and Implementation of a Brain-Computer Interface System for Lower Limb Exoskeleton Control using Deep Learning-Based Motor Imagery Classification

Sergio Manso Coloma

2025

RESUMEN

Las interfaces cerebro-computadora (BCI) representan una alternativa prometedora para restaurar funciones motoras en personas con discapacidades neuromotoras. Este trabajo se centra en el desarrollo de un sistema BCI no invasivo capaz de distinguir entre el estado de reposo y la imaginación motora (MI) de ambos pies, utilizando señales de electroencefalografía (EEG). El objetivo final es permitir el control intuitivo de un exoesqueleto de extremidades inferiores mediante la actividad cerebral voluntaria. Se implementaron tres arquitecturas de aprendizaje profundo especializadas en el EEG: EEGNet, EEG-Inception y EEGSym. Los modelos se entrenaron utilizando una estrategia de aprendizaje por transferencia, que incluyó un preentrenamiento con las bases de datos públicas PhysioNet y AlexMI, seguido de una fase de fine-tuning con un conjunto de datos propio obtenido de un solo sujeto, utilizando un sistema EEG de ocho canales. Esta configuración se eligió para facilitar su uso en aplicaciones reales. Las señales fueron preprocesadas de forma estandarizada y segmentadas en ventanas temporales de 3 segundos antes de su introducción en los modelos. La evaluación se realizó mediante métricas clásicas de clasificación: exactitud, precisión, recall, F1-score y tasa de falsos positivos (FPR) para cada clase. Ningún modelo superó el 60 % de exactitud. EEGNet mostró el mejor rendimiento general, con un equilibrio aceptable entre sensibilidad y especificidad. EEGSym resultó más sensible a la actividad de MI, aunque con más falsos positivos durante el reposo. EEGInception, en cambio, tuvo un rendimiento cercano al azar. Los resultados reflejan limitaciones clave, como la escasez de datos, la desalineación entre tareas de las bases de datos y la resolución espacial limitada derivada del bajo número de canales. Estas condiciones impidieron el aprendizaje de representaciones robustas por parte de los modelos. Además, se observó un compromiso entre la capacidad de detectar correctamente los intentos de MI y la seguridad ante falsas activaciones en reposo, lo que plantea retos para su uso en tiempo real. Este trabajo proporciona una base experimental sólida para futuros desarrollos de BCIs orientadas al control de exoesqueletos de miembro inferior. Aunque los resultados no permiten aún una implementación clínica, se identifican claramente las áreas que requieren mejora: mayor volumen de datos, alineación entre dominios, y optimización de la arquitectura de red bajo restricciones prácticas. En conclusión, este trabajo sienta las bases para futuras aplicaciones BCI en rehabilitación de miembros inferiores. Aunque los modelos actuales no alcanzan aún estándares clínicos, el marco desarrollado demuestra viabilidad técnica e identifica áreas clave de mejora en términos de datos, adaptabilidad y aplicación práctica.

PALABRAS CLAVE

Electroencefalografía (EEG), Interfaz Cerebro-Computadora (BCI), Imaginación Motora (MI), Aprendizaje Profundo (DL), Exoesqueleto, Preentrenamiento, Fine-tuning.

SUMMARY

Brain-computer interfaces (BCIs) are a promising alternative for restoring motor function in individuals with neuromotor impairments. This MSc Thesis presents the development of a non-invasive BCI system designed to classify electroencephalographic (EEG) signals to distinguish between resting state and motor imagery (MI) of both feet. The goal is to enable intuitive control of a lower-limb exoskeleton based on voluntary brain activity. Three deep learning architectures optimized for EEG: EEGNet, EEG-Inception, and EEGSym were implemented. All models followed a transfer learning strategy, they were pretrained using PhysioNet and AlexMI databases and later fine-tuned on a custom dataset recorded from a single subject using an 8-channel EEG system. This reduced-channel configuration was chosen to enhance usability in practical settings. EEG signals were preprocessed with a standardized pipeline and segmented into 3 seconds temporal windows for input into the networks. Model performance was evaluated using standard classification metrics: accuracy, precision, recall, F1-score, and false positive rate (FPR) for both rest and MI classes. No model achieved accuracy above 60%. EEGNet showed the best overall performance, with a relatively good balance between sensitivity and specificity. EEGSym was more responsive to MI signals but produced more false positives during rest. EEGInception performed at close to random. The modest results are attributed to key limitations such as data scarcity, label mismatches between datasets, and limited spatial resolution due to the low number of EEG channels. These factors prevented the models from learning strong and generalizable representations. A clear trade-off was observed between MI sensitivity and resting-state specificity, posing a challenge for real-time application. This work provides a functional and experimental foundation for future research in BCI-based lower limb exoskeleton control. While the current results do not support clinical use, the study highlights critical areas for improvement, including data volume, inter-dataset alignment, and architectural optimization under real-world constraints.

KEYWORDS

Electroencephalography (EEG), Brain-Computer Interface (BCI), Motor Imagery (MI), Deep Learning (DL), Exoskeleton, Pretraining, Fine-tuning.

TABLE OF CONTENTS

GLOSSARY OF ACRONYMS

AI	Artificial Intelligence
AR	Autoregressive Modeling
BCI	Brain Computer Interface
BLSTM	Bidirectional Long Short-Term Memory
CAN	Controller Area Network
CAR	Common Average Reference
CNNs	Convolutional Neural Networks
CSP	Common Spatial Patterns
c-VEPs	Code-Modulated Visually Evoked Potentials
DL	Deep Learning
DR	Dropout Rate
EEG	Electroencephalogram
EMD	Empirical Mode Decomposition
EOG	Electrooculography
ERD	Event-Related Desynchronization
ERP	Event-Related Potential
ERS	Event-Related Synchronization
fact	Activation Function
fMRI	Functional Magnetic Resonance Imaging
FPR	False Positive Rate
ICA	Independent Component Analysis
IMFs	Intrinsic Mode Functions
KNN	K-Nearest Neighbors
LDA	Linear Discriminant Analysis
LSL	Lab Streaming Layer
lr	Learning Rate
MEG	Magnetoencephalogram
ME	Motor Execution
MI	Motor Imagery
ML	Machine Learning
MOABB	Mother of All BCI Benchmarks
MPCA	Multiscale Principal Component Analysis
M1	Primary Motor Cortex
NIRS	Near Infra-Red Spectroscopy
PCA	Principal Component Analysis
PSD	Power Spectral Density

RNN	Recurrent Neural Network
SCPs	Slow Cortical Potentials
SMA	Supplementary Motor Area
SMRs	Sensorimotor Rhythms
STFT	Short-Time Fourier Transform
SSEPs	Steady-State Evoked Potentials
SVM	Support Vector Machines
VMI	Visual Motor Imagery
VR	Virtual Reality

LIST OF FIGURES

LIST OF TABLES

1 INTRODUCTION AND OBJECTIVES

1.1 BRAIN COMPUTER INTERFACES (BCIs)

Brain-computer interfaces (BCIs) are systems that acquire, analyze and translate brain signals into commands that are relayed to output devices that carry out desired actions. This field represents an innovative intersection between neuroscience, engineering and computer science (Shih et al., 2012). This technology possesses the capacity to fundamentally alter human interaction with digital environments, by providing novel avenues for communication and device control among individuals with profound disabilities, enhancing cognitive and sensory functions, and facilitating advanced solutions for neurorehabilitation and the monitoring of mental health (Kawala-Sterniuk et al., 2021). The concept of BCIs originated in the mid-20th century, with foundational research conducted by Jacques Vidal involving non-human primates (Vidal, 1973). Since then, significant progress in neuroimaging, signal processing, and machine learning has markedly accelerated the development and practical application of BCI technologies. A simplified representation of a BCI system's operational framework is presented in Figure 1.

1.1.1 BRAIN ACTIVITY SIGNAL ACQUISITION METHODS

The ability to understand and interact with brain activity relies fundamentally on the accurate capture of neural signals. There are several methods to acquire these signals, which are generally categorized into invasive and non-invasive techniques (Wolpaw & Wolpaw, 2012).

Invasive techniques involve surgical procedures to implant microelectrodes that record brain signals directly from the surface of the cortex. These methods allow for the recording of high-fidelity neural activity without damaging neurons. Because the electrodes are placed within the skull, they avoid signal distortion caused by the skull and surrounding tissues, resulting in finer signal quality. Moreover, invasive methods offer several advantages, including a high signal-to-noise ratio, superior spatial and temporal resolution, greater signal amplitude, enhanced resistance

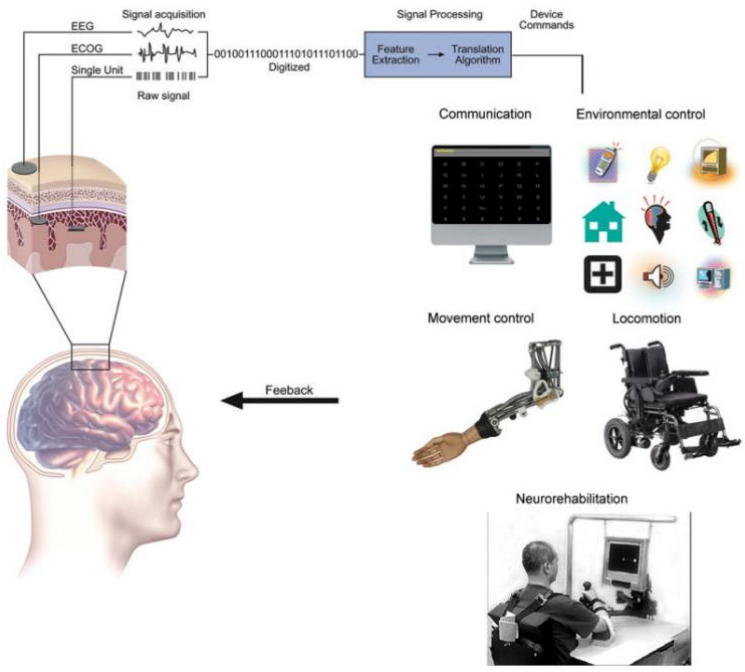

Figure 1. Typical components of a BCI system and communication methods. Simplified scheme (Kawala-Sterniuk et al., 2021).

to artifacts, and access to a wider frequency spectrum. Nonetheless, the need for surgical intervention and the associated medical risks limits their application in human subjects, thereby reducing their practicality compared to non-invasive alternatives (Wolpaw & Wolpaw, 2012).

In contrast, non-invasive techniques do not involve any surgical procedures; instead, they detect brain activity through sensors positioned on the scalp. The most widely utilized non-invasive methods are (Shih et al., 2012):

- **Near Infra-Red Spectroscopy (NIRS):** Employs near-infrared light to monitor variations in blood oxygenation and blood volume within the brain. By emitting light through the scalp and analyzing the reflected signals, NIRS captures information related to brain activity via the hemodynamic response. This technique provides relatively high spatial resolution and is notably portable, which makes it well-suited for use in naturalistic or real-world settings. However, its temporal resolution remains limited in comparison to other neuroimaging modalities.

- **Functional magnetic resonance imaging (fMRI):** Assesses brain activity by detecting changes in cerebral blood flow, utilizing magnetic fields and radiofrequency waves. This method offers exceptional spatial resolution, enabling highly detailed mapping of functional brain regions. Despite its strengths, fMRI is associated with several limitations: it is costly, characterized by low temporal resolution, and necessitates that subjects remain immobile within a large and noisy scanner. These constraints reduce their practicality for everyday BCI applications.

- **Magnetoencephalogram (MEG):** Records the magnetic fields generated by neuronal electrical activity using highly sensitive magnetometers. This non-invasive technique delivers superior spatial resolution compared to EEG, along with excellent temporal resolution, enabling precise localization of brain activity. Nonetheless, MEG systems are expensive and require operation within magnetically shielded environments, which significantly limits their accessibility and applicability in everyday or mobile contexts.

- **Electroencephalogram (EEG):** EEG is one of the most employed non-invasive techniques for measuring electrical brain activity, achieved through electrodes positioned on the scalp. EEG provides high temporal resolution, is relatively low-cost, and involves a straightforward setup, making it highly accessible for research and clinical use. Despite its advantages, EEG is characterized by limited spatial resolution and susceptibility to noise and artifacts. Nevertheless, its portability and ease of use have established it as a preferred modality in numerous BCI applications.

In the context of BCI applications, there is a particular need for systems that are portable, cost-effective, non-invasive, and easy to operate. For these reasons, EEG has become the most utilized technique in BCI research and development, making it the logical choice for implementation in the present project.

1.1.2 ELECTROENCEPHALOGRAPHY (EEG)

Brain electrical activity is generated by the transmission of postsynaptic potentials that occur simultaneously during the synaptic excitation and inhibition of millions of pyramidal neurons, which are positioned perpendicularly to the cerebral cortex (Cohen, 2017). These postsynaptic potentials are generated by ionic exchanges following the gradient direction across the cell membrane, producing ion currents, such that neurons act as tiny electrical dipoles (Sanei & Chambers, 2013). EEG is capable of measuring brain electrical activity with high temporal resolution, allowing for the observation of very precise changes in electrical activity over time (Cohen, 2017). However, this technique has low spatial resolution, displaying a limited capacity to record electrical activity from deep brain structures. The electrical activity signals captured by EEG are attenuated, spread, and contaminated by noise as they travel through the various layers of the

head. This phenomenon is known as the volume conduction effect and can lead to false correlations between the time series recorded by nearby electrodes, as they may be capturing electrical activity from the same brain sources, even if these sources are independent (Ruiz-Gómez et al., 2019).

The EEG signal is typically contaminated by artifacts that are not of interest. Among the most common are: (i) artifacts due to the power line (50/60 Hz), caused by electrical devices or poor electrode contact leading to high impedance; (ii) cardiac artifacts, produced by the electrical activity of the heart, which appear as spike-shaped waves and can be mistaken for brain electrical activity; (iii) artifacts due to muscle movement, generated by electrical activity from movements of the scalp, facial, jaw, and neck muscles; and (iv) artifacts caused by eye movements, resulting from movements of the eyeball and eyelids, producing changes in the eye potential that primarily affect the frontal electrodes (Sazgar & Young, 2019). To eliminate these artifacts and obtain an acceptable signal, EEG preprocessing is essential (Sanei & Chambers, 2013).

1.1.2.1 PHYSIOLOGICAL RHYTHMS OF THE EEG SIGNAL

EEG is traditionally divided into five frequency bands: delta (δ), theta (θ), alpha (α), beta (β), and gamma (γ). These frequency bands exhibit different amplitudes and frequencies and are typically associated with various cognitive states (Jafari et al., 2020; Sanei & Chambers, 2013). The different brain rhythms present in an EEG recording are illustrated in Figure 2.

- **Delta rhythms (δ):** These include frequencies in the 0.5–4 Hz range. They are the slowest waves but have the highest amplitude, reaching between 100 and 200 μV. They are associated with deep sleep and states of unconsciousness. δ waves may also be linked to pathological states such as loss of consciousness or coma. They are mainly located in the frontal and parieto-occipital regions.

- **Theta rhythms (θ):** These include frequencies in the 4–8 Hz range and have amplitudes between 30 and 60 μV. θ rhythms are associated with meditative states and transitions into drowsiness. They are primarily observed in the parietal, temporal, and occipital areas.

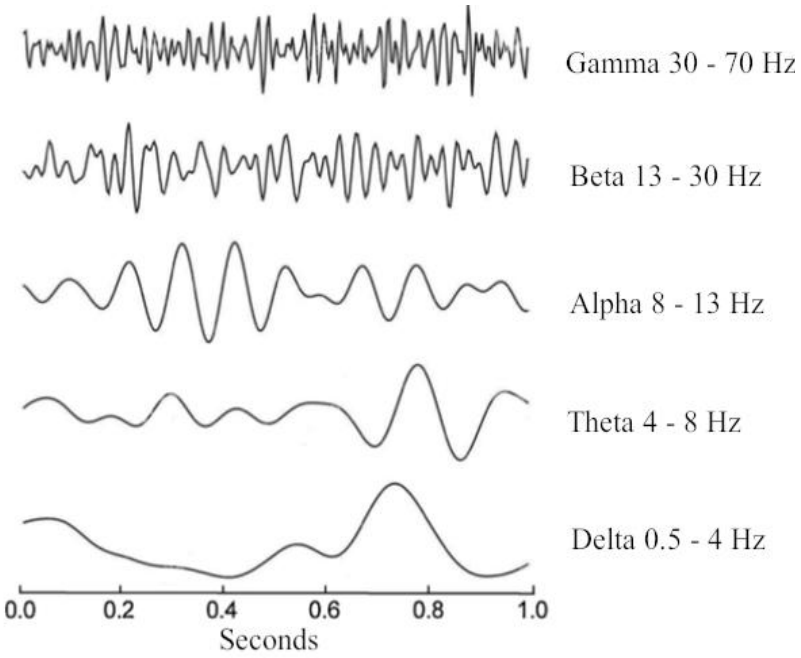

Figure 2. Brain rhythms observable in an EEG recording. Image adapted from (Jafari et al., 2020).

- **Alpha rhythms (α)**: These include frequencies in the 8–13 Hz range and can reach amplitudes of up to 50 μV. α waves are thought to indicate a relaxed state of consciousness, without focused concentration or attention. They are observed during relaxed states with closed eyes and are localized in the parieto-occipital region.

- **Beta rhythms (β):** These include frequencies in the 13–30 Hz range and have low amplitudes, between 20 and 30 μV. β waves are associated with cognitive tasks requiring concentration and with processes related to the somatomotor cortex. They predominate in the frontal and frontopolar regions. This band can be further divided into two sub-bands: β1 (13–19 Hz) and β2 (19–30 Hz).

- **Gamma rhythms (γ):** These include frequencies above 30 Hz and are the highest-frequency oscillations. They also have the lowest amplitude, between 10 and 20 μV. γ waves are related to situations involving high-level information processing. They are located mainly in the frontal and central regions.

Additionally, for this study, we are going to make use of an additional band withing the frequency of the SMR wave known as the μ band (12-15Hz), in between α and β, due to its significance in EEG systems based on Motor Imagery (MI).

1.1.2.2 EEG RECORDING

EEG recording refers to the procedure and methodology through which the brain's electrical activity is captured. This activity is measured using a series of electrodes placed on the scalp, which detect voltage fluctuations generated by neuronal activity. The number of electrodes used significantly influences the spatial resolution of the EEG signal; increasing the number of electrodes enhances spatial detail but also leads to higher computational demands and greater financial cost. While clinical recordings often utilize 19 channels, research applications may employ arrays with 8, 16, 32, 64, 128, or more electrodes (Michel & Brunet, 2019; Song et al., 2015).

To ensure consistency and reliability in electrode placement, several standardized systems are employed. The most widely adopted is the 10-20 system, illustrated in Figure 3, an international standard in which electrodes are positioned at intervals of 10% or 20% of the distance between anatomical landmarks such as the nasion and inion. Electrode labels consist of letters and numbers: the letters correspond to specific brain regions Fp (frontopolar), F (frontal), C (central), P (parietal), T (temporal), and O (occipital) while the numbers indicate hemisphere location, with odd numbers

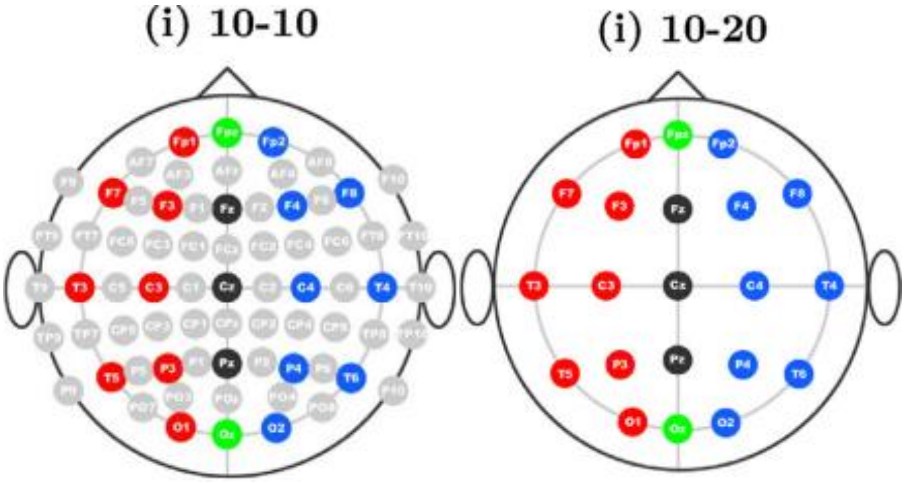

Figure 3. 10-10 and 10-20 electrode placement systems. Image adapted from (Song et al., 2015).

referring to the left hemisphere, even numbers to the right, and midline electrodes labeled with a 'z'. For higher spatial resolution, denser configurations such as the 10-10 system, illustrated in Figure 3, are used, with electrodes spaced at 10% and 5% intervals respectively (Nunez & Srinivasan, 2006).

The EEG signal recorded at each electrode site represents the difference in electrical potential between two electrodes, or between an electrode and a designated reference. The choice of reference plays a critical role due to the inherently differential nature of EEG signals. When a common reference is used, often placed at locations such as the earlobes or the vertex, the setup is referred to as a referential montage. Alternatively, in a bipolar montage, the signal reflects the potential difference between pairs of adjacent electrodes. This configuration is commonly used when the number of electrodes is limited. While both montages are widely used, each offers distinct advantages depending on the application. Referential montages provide better spatial resolution and are particularly advantageous for topographical analyses and quantitative EEG, as they allow for easier identification of the location and distribution of brain activity. However, they are highly dependent on the choice of reference, which may introduce artifacts if the reference site is not electrically neutral. In contrast, bipolar montages are more robust against common-mode artifacts and are particularly useful in clinical contexts such as epilepsy monitoring, where detecting the propagation of focal discharges is essential. Therefore, the optimal montage depends on the specific goals of the recording (Sanei & Chambers, 2013; Sazgar & Young, 2019).

1.1.3 TYPES OF CONTROL SIGNALS IN BCIs

The functionality and efficiency of BCIs are critically dependent on the nature and quality of the control signals extracted from neural activity. These signals are essential, as BCIs are not capable of detecting arbitrary brain activity; rather, they are designed to recognize specific patterns of neural responses. Consequently, engineering methodologies are required to identify and harness these patterns for practical implementation. As previously discussed, the EEG is the preferred technique for acquiring such signals. The location and number of electrodes employed for signal acquisition vary depending on the specific control signal targeted. Broadly, these control signals can be categorized into two principal classes (Ramadan & Vasilakos, 2017).

1. **Exogenous signals:** These signals are elicited in response to external stimulation. It is an involuntary response to external stimuli, which may occasionally cause discomfort to the subject.

    - *Steady-State Evoked Potentials (SSEPs):* SSEPs are neural responses that occur at a fixed frequency in reaction to continuous or repetitive stimuli, such as visual, auditory, or tactile inputs. When a user directs their attention to a stimulus that oscillates at a constant rate, the brain's electrical activity becomes synchronized with that frequency, generating detectable SSEPs, particularly within the visual cortex located in the occipital lobe.

    - *Code-Modulated Visually Evoked Potentials (c-VEPs):* In this paradigm, multiple visual stimuli are modulated using pseudorandom codes. When an individual fixates on a specific coded stimulus, a corresponding c-VEP response is elicited. This response can subsequently be decoded and employed to control the BCI system.

    - *P300 Evoked Potentials*: The P300 is a type of event-related potential (ERP) that manifests approximately 300 milliseconds after the presentation of an infrequent or significant stimulus, typically within an "oddball" paradigm. It is characterized by a positive deflection in the EEG signal and is widely utilized in BCI applications due to its robustness and ease of detection. The general structure of a BCI system based on P300 signals is illustrated in Figure 4.

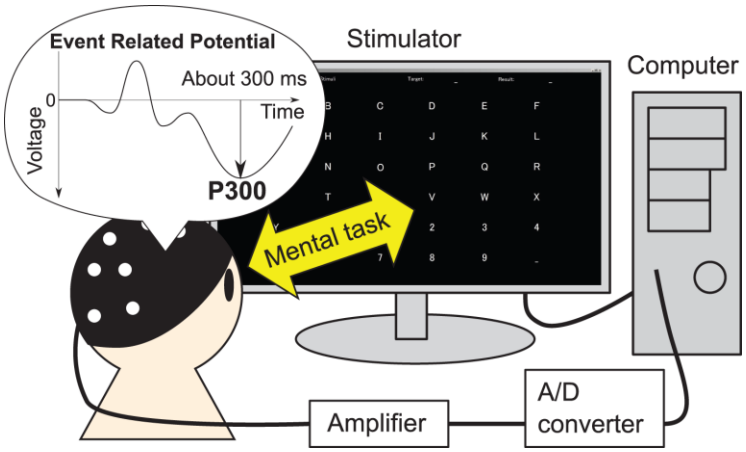

Figure 4. Structure of a P300-based BCI system. The subject engages in a mental task, enabling the BCI system to predict the intended letter (Onishi & Natsume, 2014).

2. **Endogenous signals:** Also known as spontaneous signals, represent brain activity that occurs naturally and continuously, independent of any external stimulation. Unlike evoked signals, which are elicited in response to specific events or stimuli, endogenous signals originate from the brain's intrinsic and ongoing neural dynamics.

- *Sensorimotor Rhythms (SMRs):* Sensorimotor rhythms are oscillatory patterns of brain activity predominantly observed within the α and β frequency bands over the sensorimotor cortex. These rhythms are modulated by MI, which is the mental simulation of movement and by motor execution.

- *Slow Cortical Potentials (SCPs):* Slow cortical potentials are low-frequency EEG signals, typically occurring at frequencies below 1 Hz. These signals are primarily detected in the frontal and central cortical regions and are associated with shifts in the depolarization levels of upper cortical dendrites. SCPs are characterized by very slow fluctuations in cortical activity, either positive or negative, that can last from 500 milliseconds extending up to 10 seconds.

- *Non-Motor Cognitive Tasks:* These tasks involve the use of cognitive processes rather than physical or motor activities to control BCIs. Several cognitive tasks can be utilized for this purpose, including musical imagination, visual counting, mental rotation, and mathematical computation. In a study conducted in 1990, Keirn and Aunon evaluated seven participants performing mental arithmetic, letter composition, geometric figure rotation, and visual counting tasks. Their findings demonstrated that these cognitive activities could be reliably distinguished through analysis of the subject's brainwave patterns (Keirn & Aunon, 1990).

1.1.4 STAGES OF BCI SYSTEMS

The objective of a BCI system is to interpret and translate EEG brain signals into commands that reflect the user's intentions in real time. This is achieved through a sequence of stages represented in Figure 5: (1) signal acquisition; (2) signal processing, which encompasses feature extraction and classification (Shih et al., 2012).

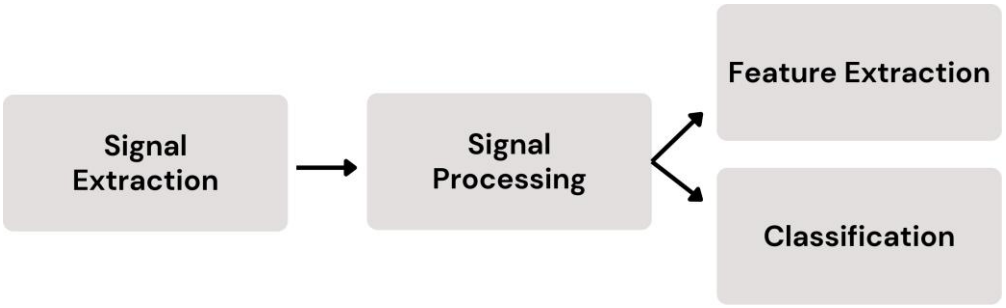

Figure 5. Stages of BCI systems

1.1.4.1 SIGNAL ACQUISITION

Signal acquisition entails the recording of brain activity using EEG sensors positioned on the scalp. As previously noted, EEG captures the brain's electrical activity, offering valuable insights into neural function. The raw EEG signals are typically of low amplitude and are therefore amplified to levels suitable for electronic processing. To enhance signal quality, filtering techniques are applied to eliminate electrical noise and other unwanted components, such as 50-Hz or 60-Hz power line interference. Following amplification and noise reduction, the signals are digitized and transmitted to a computer for subsequent processing stages.

1.1.4.2 SIGNAL PROCESSING

Signal processing involves two main steps: feature extraction and classification (Wolpaw & Wolpaw, 2012)

- Feature extraction involves analyzing digitized EEG signals to identify relevant characteristics that reflect the user's intentions. These features must be both compact and discriminative, enabling efficient translation into output commands. Given that meaningful brain activity is often transient or oscillatory in nature, commonly extracted features in contemporary BCI systems include the power within specific EEG frequency bands, as well as the amplitude and latency of EEG responses.

- Classification algorithms are responsible for translating the extracted EEG features into executable application commands. This translation may be achieved through direct mappings, threshold-based decision rules, or more sophisticated machine learning classification methods. Importantly, the translation mechanism must be dynamic and adaptable to spontaneous or learned variations in signal features. Such adaptability ensures that the system can accommodate the full range of the user's potential neural patterns for effective and reliable device control.

Machine Learning (ML), a subfield of artificial intelligence (AI), is dedicated to developing algorithms capable of learning from data and making informed decisions or predictions. However, traditional ML techniques are subject to notable limitations, including the need for extensive and labor-intensive manual feature engineering, as well as high computational demands that may still fall short in capturing complex patterns within neural data (Kamath et al., 2018).

Deep Learning (DL) is an advanced subfield of machine learning that employs neural networks with multiple layers known as deep neural networks to model and analyze complex data patterns. In the context of BCI signal processing, DL techniques are increasingly utilized to enhance both feature extraction and classification processes (Iftikhar et al., 2018). Models such as convolutional neural networks (CNNs) and recurrent neural networks (RNNs) are particularly prominent due to their capacity to autonomously learn and extract sophisticated features directly from raw EEG signals. Unlike conventional ML approaches, which depend heavily on manual feature engineering,

DL enables end-to-end optimization of the entire processing pipeline. This capability is especially beneficial for capturing the complex temporal dynamics and spatial dependencies embedded in EEG signals that are associated with user intent (Liu et al., 2019).

By leveraging DL, BCI systems can attain improved accuracy and robustness in translating brain signals into meaningful commands. This approach also enhances the system's ability to adapt to individual users, as DL models can be trained on personalized datasets, allowing the system's responses to be finely tuned to the unique neural patterns of each user. In conclusion, deep learning constitutes a major advancement in the evolution of more sophisticated and efficient BCI systems, offering the potential for interfaces that are both more intuitive and highly responsive.

1.1.5 APPLICATIONS OF BCI

BCI systems have a broad spectrum of applications across diverse fields, enabling the translation of brain activity into actionable commands. These applications range from clinical and therapeutic interventions to non-medical contexts, enhancing quality of life and introducing novel modes of human-computer interaction. These systems can be classified based on the nature of user involvement in generating brain activity, commonly categorized as active or passive systems. An active BCI requires deliberate user engagement, wherein the user intentionally modulates brain activity to control the system. Conversely, a passive BCI infers the user's cognitive or affective states by analyzing ongoing brain activity, without requiring intentional control. Additionally, active BCIs may rely on neural responses elicited by external stimuli (Sibilano et al., 2024). Hereafter, we briefly outline some of the most significant applications of BCI technology (Padfield et al., 2019; Wolpaw & Wolpaw, 2012).

- **Assistive Technologies for Individuals with Disabilities:** One of the most prominent and intuitive applications of BCIs in the medical field is in assistive technologies for individuals with severe physical impairments. BCIs can enhance the autonomy of these individuals by providing alternative methods to interact with their environment. For instance, users can operate wheelchairs, control prosthetic limbs, or manage home automation systems using only their brain activity. Such capabilities contribute significantly to improving both physical independence and psychological well-being. A particularly impactful application is found in supporting individuals with locked-in syndrome, a condition characterized by the near-total loss of voluntary muscular control. For these patients, BCIs offers a critical communication channel by detecting brain signals associated with specific thoughts or intentions (Branco et al., 2021). These signals can then be used to select letters, words, or phrases on a computer screen, enabling meaningful interaction with others. This form of communication dramatically enhances the quality of life for patients who would otherwise lack any means of interaction or expression (Milekovic et al., 2018).

- **Endogenous Cerebral Stimulation and Neurofeedback:** Passive BCI systems offer significant potential in the realm of cognitive state monitoring, particularly for managing mental workload. By continuously assessing neural activity, these systems can infer cognitive states such as attention, fatigue, or engagement. This information can be utilized to optimize various environments, for instance, adapting workspaces for improved productivity or tailoring educational content to individual learners. In the educational context, BCIs have been employed to monitor students' levels of attention and comprehension, enabling instructors to dynamically adjust teaching strategies for enhanced effectiveness (Baldwin & Penaranda, 2012). Furthermore, when integrated with pedagogical methods, BCIs can support skill acquisition and performance enhancement, ultimately leading to improved academic outcomes (Jamil et al., 2021). Beyond adaptive learning, active BCIs have shown promise in memory training. For example, Lee et al. developed a BCI-based intervention that utilized EEG patterns to improve various

cognitive functions, including immediate and delayed memory, as well as visuospatial and constructional attention (Lee et al., 2013). Other studies have targeted cognitive enhancement in older adults; Gomez-Pilar et al., for instance, demonstrated that tasks involving MI could improve visual perception, expressive language, and short-term memory (Gomez-Pilar et al., 2014).

- **Entertainment, Gaming, and Virtual Reality (VR):** The integration of BCIs into gaming and virtual reality environments introduces novel forms of immersive and interactive experiences. By enabling users to control virtual characters or interact with digital environments through brain signals, BCIs elevate the level of user engagement beyond traditional input methods. These systems allow virtual platforms to respond dynamically to users' cognitive states and intentions, fostering a more personalized and responsive experience. Beyond entertainment, such applications also hold potential therapeutic value, offering engaging tools for cognitive training, rehabilitation, or emotional regulation through gamified environments (Yadav et al., 2020).

1.1.5.1 PROSTHETIC LIMBS AS AN ASSITIVE TECHNOLOGY

Recent advances in BCI technologies have opened new possibilities for the intuitive control of prosthetic limbs by directly decoding motor intention from brain activity. Unlike traditional systems that rely on residual muscular activity, BCIs bypasses the peripheral nervous system and allows users to control external devices using only neural signals, typically recorded non-invasively through EEG. One of the most widely explored paradigms for BCI-based control is MI, the mental simulation of movement without actual execution. MI tasks produce detectable modulations in sensorimotor rhythms (SMRs), particularly in the mu and beta frequency bands, which can be decoded in real time to generate control commands (Wolpaw & Wolpaw, 2012). This strategy has been extensively applied in upper-limb prosthetics, where users can control robotic arms or hand prostheses to perform goal-directed tasks such as grasping, lifting, or rotating (Lebedev & Nicolelis, 2006). These systems have shown promising results in both healthy subjects and individuals with amputations or neurological damage.

In contrast, the application of BCI to lower-limb prostheses is less developed, largely due to increased biomechanical complexity and more challenging signal acquisition. The cortical areas responsible for lower-limb movement lie deep within the interhemispheric fissure, making it harder to access with EEG. Moreover, gait control involves continuous and cyclic coordination, requiring more sophisticated decoding approaches than the discrete gestures typically used in upper-limb systems. Despite these challenges, emerging studies have demonstrated the feasibility of detecting gait intention, step events, and movement onset from EEG signals, with applications in both prosthetic control and robotic exoskeletons for rehabilitation (Chaudhary et al., 2016; Miguel-Fernández et al., 2023). Lower-limb exoskeletons are gaining traction as promising platforms for integrating BCI-based control in the context of neurorehabilitation. These wearable robotic systems assist or amplify lower-limb movement during walking, and their use in conjunction with MI-based BCIs allows for the closed-loop engagement of neural circuits involved in gait control. Such systems not only support mobility in users with impaired motor function but also offer a therapeutic benefit by stimulating motor cortical areas during rehabilitation training. The combination of BCIs and exoskeletons holds great potential for restoring volitional gait control in individuals with neurological disorders (Miguel-Fernández et al., 2023).

1.2 HYPOTHESIS

BCI systems offer a promising approach for controlling assistive devices in individuals with motor impairments. BCIs based on MI not only provides a control mechanism for assistive devices but also stimulate cortical reorganization and functional recovery. Typically, these systems rely on the EEG to capture brain activity, often using many channels, which is often time-consuming for

real-world or clinical applications. Moreover, it has been shown that the use of DL can enhance the accuracy and robustness of BCIs in decoding brain signals into meaningful commands. Nevertheless, the control of lower-limb prostheses via BCIs remains relatively underexplored.

1.3 OBJETIVES

This Master Thesis proposes the design and implementation of a BCI system for controlling a lower-limb exoskeleton based on three different DL models for MI classification, using only eight EEG channels. To achieve this, the following specific objectives are proposed:

i. To conduct a state-of-the-art review on BCI, EEG, DL and MI.

ii. To analyze public BCI databases with EEG recordings of MI trials of the gait.

iii. To register EEG recordings of MI trials of the gait

iv. To preprocess the EEG signals and train the different DL models with EEG trials.

v. To perform a real time classification of new EEG signal trials in either a walking or resting state.

vi. To connect the output of the DL models with the exoskeleton for real time control.

vii. To analyze and discuss the results obtained, as well as identify limitations and propose future lines of research.

1.4 STRUCTURE OF THE STUDY

This section defines the structure of this MSc Thesis, which consists of nine chapters. Each of them is listed and briefly described below.

- **Chapter 1. Introduction and objectives.** This chapter provides an overview of BCIs, including signal acquisition methods with a focus on EEG as well as types of control signals, BCI processing stages, and potential applications. It also presents the motivation behind the study, the central hypothesis, and the specific objectives of the project.

- **Chapter 2. Motor Imagery based BCIs.** This chapter explores the principles of MI and its neural correlations. It details the generation and modulation of SMRs, strategies for EEG-based MI detection, and the application of deep learning models to decode EEG signals for MI classification.

- **Chapter 3. Materials and Methods.** This section outlines the methodology used in the study, including participant information, the EEG acquisition, the employed databases, the experimental paradigm, and signal preprocessing techniques. It also describes the implementation and evaluation of three deep learning models: EEGNet, EEG-Inception, and EEGSym, as well as the connection with the lower-limb exoskeleton.

- **Chapter 4. Results.** This chapter presents the results and evaluation obtained from training and evaluating the selected models. Performance metrics are reported to support the analysis.

- **Chapter 5. Discussion.** The findings are critically interpreted, with comparisons made to existing literature. The implications of the results are discussed in the context of BCI-based exoskeleton control and potential clinical applications.

- **Chapter 6. Conclusion and future work.** This chapter summarizes the main conclusions of the study and assesses the extent to which the proposed objectives have been met. Additionally, it identifies limitations and suggests future research directions to further improve the system.

- **Chapter 7. Ethical, Economic, Societal and Environmental aspects.** This section evaluates the project's broader impacts, including ethical considerations, sustainability, accessibility, and societal benefits, in accordance with the institutional requirements for responsible engineering practice.

- **Chapter 8. Financial Budget.** An estimated financial budget is presented, detailing personnel costs, equipment depreciation, consumables, and indirect costs.

- **Chapter 9. Bibliography.** This final section contains the list of all scientific literature and sources cited throughout the document.

2 MOTOR IMAGERY BASED BCIs

2.1 PARADIGM

MI-based BCIs operate by detecting characteristic patterns of brain activity elicited during the mental simulation of movement. By decoding the brain's electrical activity associated with imagined motor tasks, these systems offer an alternative channel for human-computer interaction that circumvents conventional neuromuscular routes. This section examines the underlying mechanisms, practical implementations, and recent developments in MI-based BCIs, emphasizing their transformative potential in the fields of neurorehabilitation and assistive technology.

2.1.1 BRAIN DYNAMICS DURING MOTOR EXECUTION

Motor execution (ME) engages a complex network of neural processes responsible for initiating, coordinating, and regulating voluntary movement. Central to ME is the activation of specific brain regions that interact dynamically to generate and modulate motor output, as illustrated in Figure 6. The main regions which play integral roles in these neural processes are (Purves et al., 2001; Wolpaw & Wolpaw, 2012):

- **Primary motor cortex (M1):** located in the precentral gyrus of the frontal lobe, is the principal cortical region responsible for generating the neural commands that govern voluntary movement. During both the planning and execution phases of motor activity, pyramidal neurons within M1 exhibit bursts of high-frequency firing. These neurons are distinguished by their long axons, which extend through the corticospinal tract to form synapses with motor neurons in the spinal cord. M1 is organized somatotopically, meaning that distinct anatomical regions within the cortex correspond to specific body parts. During motor execution, neuronal populations within the relevant M1 region increase their firing rates, initiating the movement of the corresponding body segment. This increase in neural activity leads to desynchronization, characterized by a reduction in power when activity is increased. M1 integrates a multitude of excitatory and inhibitory synaptic inputs for producing smooth and coordinated motor outputs. Excitatory and inhibitory postsynaptic potentials summate to modulate the firing rate of motor neurons, allowing for the precise regulation of muscle contraction required for voluntary motion.

- **Premotor Cortex and Supplementary Motor Area (SMA):** The premotor cortex, situated anterior to the primary motor cortex, plays a key role in the planning and coordination of voluntary movements. This region contributes to motor preparation by integrating sensory inputs with motor intentions, thereby facilitating the selection of appropriate motor responses based on external cues. Complementing its function, the SMA, located on the medial surface of the frontal lobe, is critically involved in the initiation and coordination of complex motor actions. It is particularly important for internally generated movements, including those that involve sequential execution or bilateral coordination. This region is essential for tasks that require the simultaneous use of both sides of the body, with neurons that exhibit preparatory activity even before the movement begins, indicating their role in movement planning.

- **Basal Ganglia and Cerebellum:** The basal ganglia comprise a group of subcortical nuclei that are essential for the initiation and modulation of movement, as well as the suppression of involuntary or inappropriate motor actions. These structures play a pivotal role in motor learning and in the execution of smooth, goal-directed movements. Neuronal activity within

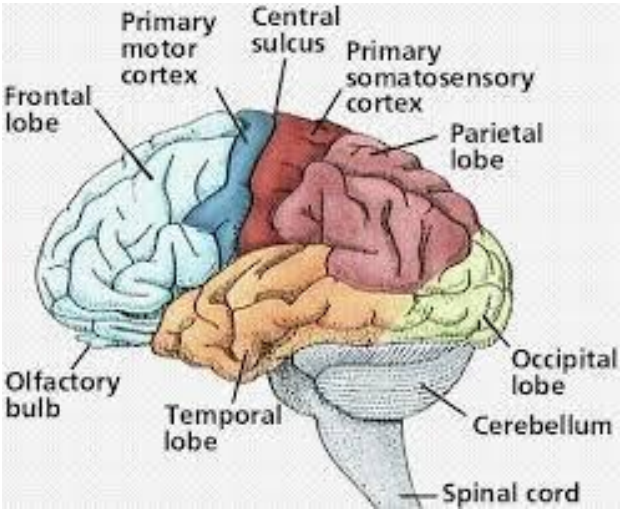

Figure 6. Cortical Areas of Human Brain (Zippo, 2011).

the basal ganglia reflects the intricate decision-making processes underlying the initiation of voluntary motion. In contrast, the cerebellum is primarily responsible for the fine-tuning of motor activity, as well as the coordination and maintenance of balance. It integrates sensory input and information from various brain regions to dynamically adjust motor output in real time.

- **Motor Pathways:** The corticospinal tract constitutes the principal conduit for motor commands transmitted from the cerebral cortex to the spinal cord. This tract conveys neural impulses originating in the motor cortex to lower motor neurons located within the spinal cord, which in turn innervate skeletal muscles. Complementing this pathway, the corticobulbar tract carries motor signals from the cortex to the brainstem, thereby governing voluntary movements of the face, head, and neck.

The coordinated activity of neurons within motor-related cortical regions, along with the modulation of cortical oscillatory rhythms, can be effectively captured through EEG, providing valuable insights into the neural mechanisms underlying motor control. Notably, during movement execution, the μ and β rhythms are prominently observed over the sensorimotor cortex. These rhythms are closely associated with the representation of the current motor state and the suppression of the initiation of new movements.

2.1.2 SENSORIMOTOR RYTHMS

SMRs are neural oscillations observed over sensorimotor cortical areas, particularly within the posterior frontal and anterior parietal regions (Wolpaw & Wolpaw, 2012). These rhythms are commonly captured via EEG, which typically records activity in the μ and β frequency bands. In contrast, more invasive or sensitive modalities such as electrocorticography and MEG can detect higher-frequency components with greater spatial and temporal precision. Within these frequency ranges, the amplitude of local oscillatory activity in the pericentral cortex markedly decreases or may be almost entirely suppressed during movement of the corresponding body part. Notably, this attenuation occurs irrespective of whether the movement is voluntary, passive, or reflexive. This phenomenon, characterized by a reduction in rhythmic synchronization during motor activity, is referred to as event-related desynchronization (ERD). ERD is typically followed by a rebound or increase in rhythmic activity after the termination of movement, known as event-related synchronization (ERS) (Pfurtscheller et al., 2006).

2.1.3 SMR DURING MOTOR BEHAVIOURS

Empirical studies have demonstrated that voluntary motor actions are consistently associated with ERD in μ and β frequency bands, localized over sensorimotor cortical regions. The μ rhythm exhibits two distinct ERD patterns: a lower-frequency, spatially widespread desynchronization, reflecting general motor preparation and attentional engagement, and a higher-frequency, topographically specific desynchronization that is closely linked to the motor task being performed. In parallel, β rhythms typically undergo desynchronization during movement execution, followed by a transient increase in synchronization post-movement, a phenomenon commonly referred to as the *β rebound* (Wolpaw & Wolpaw, 2012).

A representative example of these dynamics can be observed in tasks involving finger flexion. Prior to movement onset, μ ERD emerges over the contralateral Rolandic cortex, indicating preparatory and attentional processes. As the movement is executed, the ERD becomes bilaterally distributed, reflecting the integration of motor planning and execution processes (Pfurtscheller et al., 2006). Importantly, this localized ERD is often accompanied by ERS in adjacent cortical regions, a phenomenon described as the *focal ERD/surround ERS*. For instance, Gerloff et al. reported that μ ERD elicited by repetitive finger movements was accompanied by increased synchronization of α rhythms in the parieto-occipital cortex, specifically within visual processing areas, suggesting task-dependent redistribution of cortical resources (Gerloff et al., 1998).

MI elicits similar modulations of SMRs. Imagined limb movements induce ERD patterns in both μ and β bands over the contralateral sensorimotor cortex, closely resembling those observed during actual physical movement. These parallels in neural activity between executed and imagined movement have been substantiated in studies involving both neurologically intact individuals and patients with motor impairments, underscoring the potential of MI as a tool for BCI-driven neurorehabilitation (Neuper et al., 2009; Pfurtscheller et al., 2006).

2.1.4 EEG-BASED STRATEGIES TO DETECT MI

Over the past decades, various EEG-based methodologies have been developed to robustly detect and interpret SMR signals. These approaches are generally categorized into three main strategies: Operant Conditioning, Machine Learning, and Adaptive Systems, each characterized by distinct conceptual frameworks and practical implementations (Ang & Guan, 2017).

- **Operant conditioning** involves training users to voluntarily modulate specific EEG features through iterative practice and feedback. In this paradigm, users learn to self-regulate their SMRs such as μ and β rhythms by receiving continuous real-time feedback from the BCI system, thereby gaining insight into how their MI influences cortical activity. This approach typically relies on a fixed signal processing pipeline, incorporating predefined parameters for EEG feature extraction, selection, and translation into control commands. As illustrated in Figure 7, this training protocol enables users to gradually shape their brain activity in a goal-directed manner. This strategy has proven effective in various BCI applications, including the control of two-dimensional cursor movement and robotic limb operation. For example, users have successfully learned to manipulate horizontal and vertical cursor trajectories by modulating μ and β rhythms, respectively, providing compelling evidence of the practical viability of this approach in real-time control systems (Wolpaw & McFarland, 2004).

- **Machine Learning** illustrated in Figure 8 addresses the variability inherent in EEG signals and mitigates the extensive training demands associated with operant conditioning. This method entails the development of a subject-specific model during a preliminary calibration phase, which is subsequently employed for MI detection. Machine learning techniques enable the customization of the BCI model to individual users by leveraging their calibration data. Algorithms such as Common Spatial Patterns (CSP) are utilized to enhance the signal-to-noise ratio, thereby improving the accuracy of MI detection (Blankertz et al., 2008).

- **Adaptive Systems** aim to address the non-stationary nature of EEG signals by continuously updating the subject specific model during system use. As illustrated in Figure 9, this approach ensures that the BCI system maintains its effectiveness even as the user's EEG patterns evolve over time. Adaptation can be implemented through supervised or unsupervised learning methods, targeting components such as spatial filters, feature selection, or classifier parameters. A co-adaptive framework enables mutual adjustment between the user and the model, thereby enhancing the system's ability to discriminate brain activity over time (Faller et al., 2014). While adaptive strategies have demonstrated potential for improving classification accuracy, particularly in real-time scenarios, their efficacy within the context of BCI-based rehabilitation remains limited (Nicolas-Alonso et al., 2015).

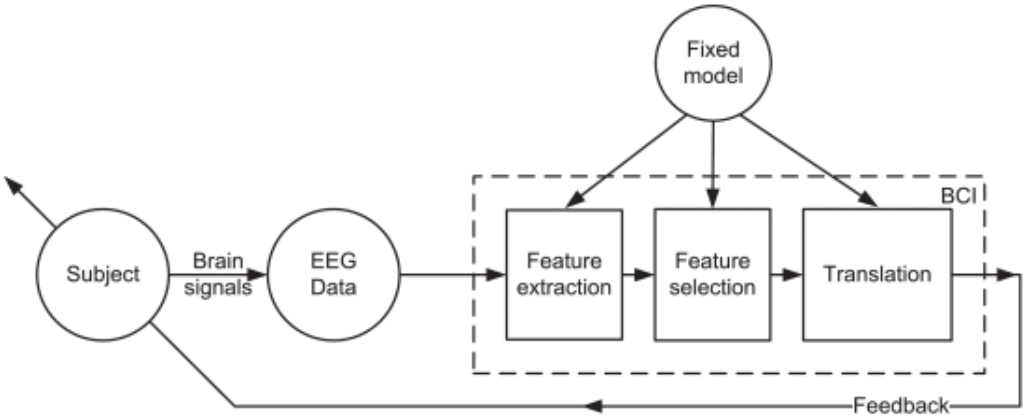

Figure 7. Operant Conditioning strategy scheme (Ang & Guan, 2017).

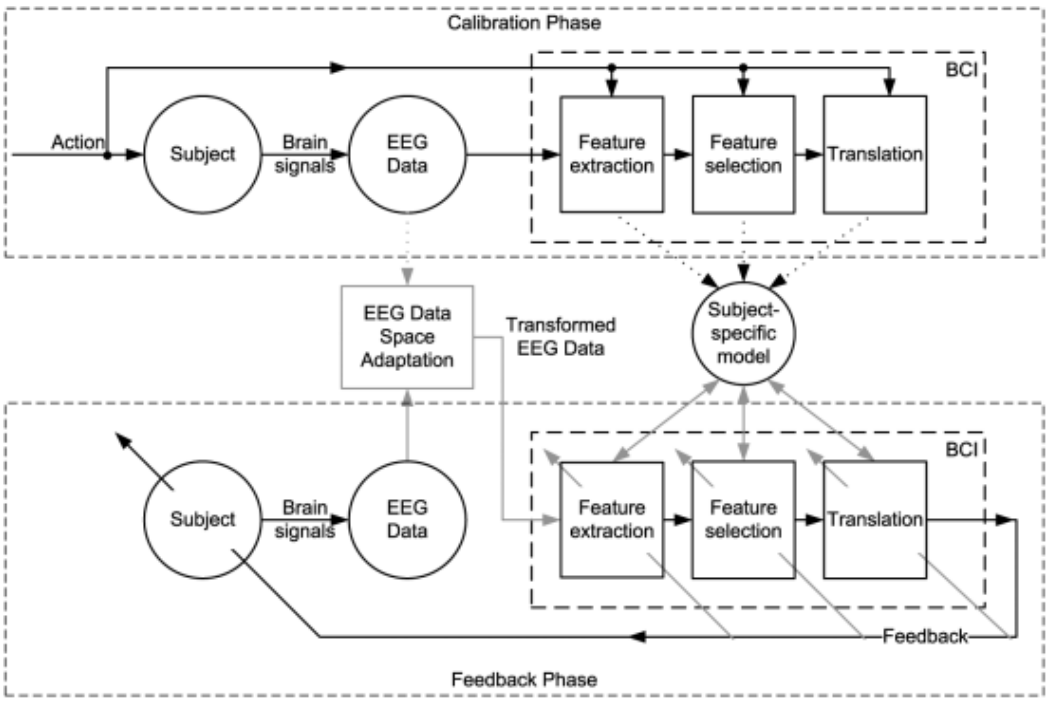

Figure 8. Machine Learning strategy scheme (Ang & Guan, 2017).

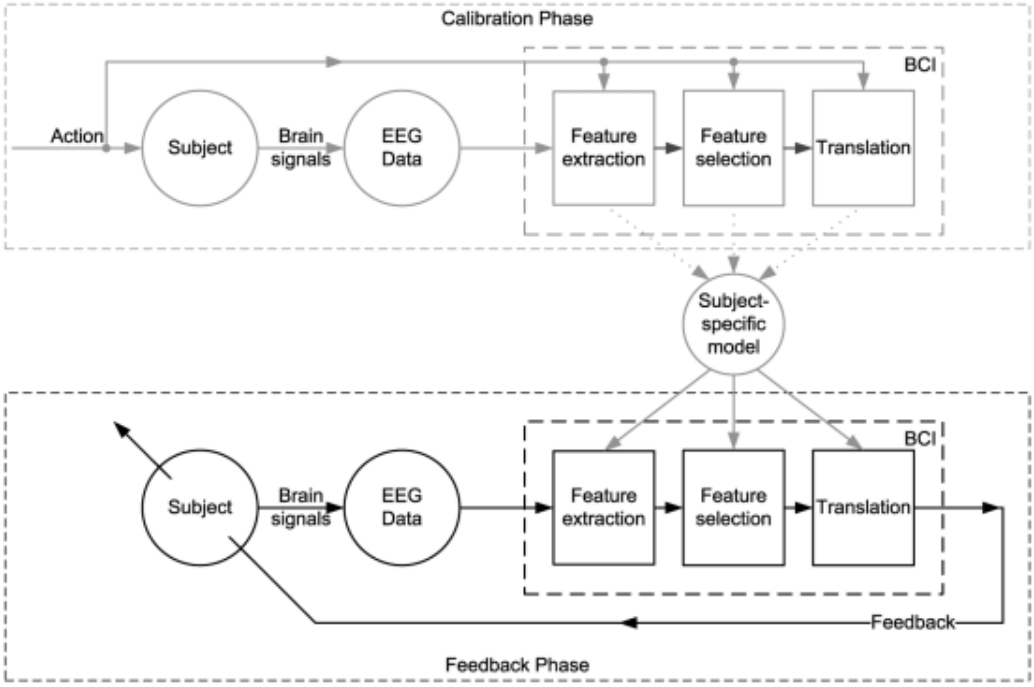

Figure 9. Adaptative strategy scheme (Ang & Guan, 2017).

2.1.5 SIGNAL PROCESSING PIPELINE FOR MI-BASED BCIs

SMR EEG signals are widely used in BCI systems due to their naturally occurring discriminative properties and the relatively low cost of signal acquisition. These signals offer valuable insights into the user's intended motor actions without necessitating actual physical movement, making them ideal for various applications, including the control of prosthetic limbs. Nevertheless, the processing of SMR EEG data poses several significant challenges. The signals, often collected from limited training sessions due to the time-consuming and demanding nature of the training process for participants, are inherently unstable and highly susceptible to noise and artifacts, complicating accurate classification. Additionally, the high dimensionality of multichannel EEG data necessitates robust feature extraction and selection techniques to maintain reliable system performance. Many classification algorithms also fail to incorporate the temporal dynamics of EEG signals, which are critical for enhancing classification accuracy. Moreover, the neurophysiological and psychological state of the user, including factors such as attention, fatigue, and inter-individual variability in brain activity can substantially influence BCI performance (Lotte et al., 2007).

In the context of raw EEG data processing, signal events are often identified using data that has been averaged across subjects or trials. While this approach can enhance signal clarity, it may also obscure instances of poor performance by masking variability through averaging. In contrast, other studies emphasize the analysis of single-trial data, thereby avoiding the aggregation across trials. This methodology is particularly valuable, as it enables the examination of performance variability on a per-trial basis and provides nuanced insights into underlying neural activity (Padfield et al., 2019). The pipeline for the processing of these signals is illustrated in Figure 10.

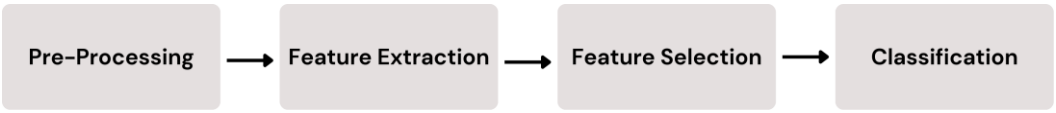

Figure 10. Signal Processing Pipeline for MI-Based BCIs.

2.1.5.1 PRE-PROCESSING

Pre-processing of EEG signals typically involves multiple steps aimed at enhancing signal quality and reliability.

- **Artifact Removal:** This step focuses on eliminating non-neural signals, including eye blinks, muscle activity, and other physiological or environmental artifacts. Common techniques include the following (Jiang et al., 2019).

  - **Independent Component Analysis (ICA)**: ICA is extensively used to decompose EEG signals into statistically independent components, facilitating the identification and removal of artifacts. By exploiting the statistical independence of underlying sources, ICA enables the isolation of components associated with artifacts, which can then be selectively excluded. However, due to its computational complexity and latency, ICA is primarily suitable for offline analysis and is generally not applicable in real-time scenarios.

  - **Regression-Based Methods**: These techniques utilize reference signals derived from known artifact sources such as electrooculography (EOG) recordings for eye movements to estimate and subtract the artifact contribution from the EEG data, thereby improving signal fidelity.

- **Filtering:** Following artifact removal, filtering is applied to eliminate frequency components that are not relevant to the analysis. This typically includes bandpass filtering to isolate specific frequency bands of interest, which are selected based on the study's objectives. In the case of SMR detection, filters are generally designed to target the μ and β frequency bands. Additionally, a notch filter usually set at 50 Hz or 60 Hz depending on the local power line frequency is employed to suppress line noise originating from electrical sources. In multichannel EEG data, spatial filtering is also commonly used to enhance the signal-to-noise ratio and to isolate neural signals arising from specific brain regions. One widely used spatial filtering technique is the Common Average Reference (CAR), which involves subtracting the mean signal across all electrodes from each individual electrode's signal. This approach helps to reduce spatially correlated noise and enhances the localization of brain activity (Wolpaw & Wolpaw, 2012).

- **Segmentation**: This stage involves dividing the continuous EEG signal into discrete epochs or time windows that correspond to specific events or task-related intervals. Segmentation is a critical step for enabling context-dependent analysis of EEG data. In MI-based BCIs, segmentation is typically synchronized with the onset and duration of MI instructions given to the user. These tasks are often designed to occur within defined temporal intervals to allow for the extraction of relevant EEG segments. For instance, Zich et al. employed time windows ranging from 2 to 4 seconds, with segmentation commonly performed in the interval between 2.5 and 4.5 seconds after task onset. Additionally, segmentation may also include the period preceding task onset, for example, between 3.5 and 0.5 seconds before the fixation cue, allowing for the examination of anticipatory brain activity (Zich et al., 2015).

- **Normalization**: Although not universally applied, normalization is often employed depending on the specific requirements of a study. This process standardizes EEG data commonly through

z-score normalization to ensure comparability across different channels and trials. Given the non-stationary nature of EEG signals, which can vary significantly between recording sessions, direct comparison of raw data is challenging. Normalization addresses this issue by transforming the data into a standardized distribution with a mean of zero and a standard deviation of one. This step is particularly critical in multichannel EEG configurations, as it helps mitigate discrepancies in signal amplitude across channels, thereby enhancing the reliability of subsequent analyses (Wolpaw & Wolpaw, 2012).

In addition to standard EEG pre-processing techniques, various studies have proposed advanced methods aimed at enhancing the accuracy and robustness of BCI systems. One such approach is Multiscale Principal Component Analysis (MSPCA), which integrates the advantages of Principal Component Analysis (PCA) with wavelet transformation. This method enables the decomposition of EEG signals across multiple scales, thereby improving artifact removal while preserving the sharp transitions and transient features that are characteristic of neural activity (Kevric & Subasi, 2017; Padfield et al., 2019).

2.1.5.2 FEATURE EXTRACTION

Following signal pre-processing, the extracted features must effectively represent salient characteristics of the EEG signal, providing a foundation for differentiating between brain states associated with specific MI tasks. Several well-established feature extraction techniques commonly employed in MI-based BCIs are (Padfield et al., 2019).

- **Time-Domain Features:** Autoregressive (AR) modeling is a widely used approach for time-domain EEG feature extraction. It entails fitting an AR model to segments of EEG data, with the resulting AR coefficients or spectral estimates serving as discriminative features. Additional time-domain metrics include root mean square and integrated EEG amplitude measures.

- **Frequency-Domain Features:** These techniques involve converting the EEG signal into the frequency domain to examine its spectral characteristics. Common methods include:

  - **Power Spectral Density (PSD):** This quantifies the distribution of signal power across various frequency components, aiding in the identification of dominant rhythms associated with cognitive or motor states.

  - **Band Power Analysis:** This approach computes the power contained within defined frequency bands. For MI-related applications, particular attention is given to the α, μ, and β bands due to their established relevance.

  - **Fourier Transform:** By transforming the time-domain signal into its constituent frequency components, the Fourier transform provides a comprehensive view of the signal's spectral content.

- **Time-Frequency Domain Features:** Given the non-stationary nature of EEG signals, features capturing both temporal and spectral information are particularly valuable:

  - **Short-Time Fourier Transform (STFT):** This method segments the EEG signal into short time windows and applies the Fourier transform to each, facilitating a temporally localized frequency analysis.

- ❖ **Wavelet Transform:** This technique decomposes the EEG signal into time-frequency representations at multiple scales, enabling the detection of transient phenomena and localized spectral changes.

- ❖ **Empirical Mode Decomposition (EMD):** EMD is a data-driven technique that decomposes the EEG signal into a set of intrinsic mode functions (IMFs), each representing a fundamental oscillatory component. Its adaptive nature makes it especially suitable for analyzing non-linear and non-stationary signals like EEG.

- **Spatial Features:** These features leverage the multi-channel configuration of EEG recordings to extract information related to the spatial distribution of neural activity across the scalp.

  - ❖ **Common Spatial Patterns (CSP):** CSP is a widely adopted spatial filtering technique that enhances class discrimination by maximizing the variance difference between two classes of EEG signals. It is particularly prevalent in MI-based BCI systems due to its effectiveness in isolating class-specific spatial patterns.

  - ❖ **Filter Bank Common Spatial Patterns (FBCSP):** FBCSP extends the standard CSP approach by applying it across multiple frequency bands. The EEG signal is first decomposed into several sub-bands using a filter bank, after which CSP is applied to each band individually. The features extracted from all sub-bands are then concatenated to form a comprehensive feature vector, enhancing the model's ability to capture task-relevant information and improving classification performance.

  - ❖ **Riemannian Geometry-Based Methods:** These methods represent the covariance matrices of multichannel EEG data as points on a Riemannian manifold. By employing tools from differential geometry, distances and features can be calculated more accurately within this non-Euclidean space. Such representations enable the extraction of robust features for EEG classification, particularly in scenarios involving inter-trial variability and noise.

- **Event-Related Features:** ERD and ERS offer insights into the dynamic modulation of brain rhythms associated with motor-related cognitive processes. Temporal analysis of ERD and ERS focuses on the timing of EEG power changes, capturing the neural dynamics associated with motor preparation, execution, and termination. Spectral analysis highlights specific frequency bands, most notably the μ and β rhythms, which exhibit power reductions during MI (ERD) and subsequent increases following task completion (ERS). Time-frequency representations, such as spectrograms, enable the visualization of how power in various frequency bands evolves over time. These representations facilitate the identification and interpretation of ERD and ERS events within specific temporal windows, contributing to a more nuanced understanding of motor-related neural activity.

2.1.5.3 FEATURE SELECTION AND CLASSIFICATION

Feature selection is a critical step aimed at identifying the most informative attributes from the extracted dataset to enhance the performance of classification algorithms. This process serves to reduce computational demands while simultaneously improving classification accuracy. Commonly employed techniques include PCA, filter bank optimization, and evolutionary algorithms. These methods systematically evaluate and retain the features that contribute most significantly to discriminative power, while eliminating those that are redundant or irrelevant.

The classification stage in MI-based EEG brain-computer interfaces involves the application of machine learning algorithms to assign the selected features to specific MI classes. A variety of classifiers have been utilized in this context, each with distinct strengths depending on the characteristics of the data and the nature of the task (Padfield et al., 2019).

- **Linear Discriminant Analysis (LDA):** LDA is a widely used classifier due to its simplicity and computational efficiency. It performs well in low-dimensional feature spaces and is effective when the classes are linearly separable.

- **Support Vector Machines (SVMs):** SVMs are particularly well-suited for high-dimensional datasets and are known for their robustness against overfitting, especially when using kernel functions to map data into higher-dimensional spaces.

- **k-Nearest Neighbors (k-NN):** This non-parametric method classifies data based on the majority label among the nearest neighbors. While conceptually simple and effective in low-dimensional settings, its computational cost increases significantly with larger datasets or higher feature dimensionality.

- **Recurrent Neural Networks (RNNs):** RNNs are designed to model sequential data and are therefore well-suited for EEG time-series classification. They can capture temporal dependencies within the EEG signals, which is critical for accurate interpretation of dynamic neural activity.

- **Deep Learning Methods:** CNNs have emerged as powerful tools for EEG classification tasks. They integrate feature extraction, selection, and classification into a unified architecture, making them especially effective for learning complex spatial and temporal patterns from raw EEG data. The following section will provide a more detailed examination of this approach.

2.1.6 BCI USES OF SMRs

The use of SMRs in BCI systems has evolved through various strategies, all grounded in the principle that SMRs undergo modulation during both actual and imagined motor activity. Typically, users engage in MI mentally simulating specific movements, which induces measurable changes in SMR amplitude. These changes are then translated into system outputs, such as cursor movement or other control commands.

While SMR-based BCIs commonly rely on MI, they differ significantly in how this mental strategy is integrated into system functionality. In some systems, it serves primarily as an initial control mechanism, enabling the user to establish communication with the interface. Over time, these systems facilitate mutual adaptation between the user and the BCI, leading to more intuitive and automatic control that becomes less reliant on explicit imagery. Conversely, other systems require continuous use of specific imagery or cognitive tasks throughout their operation, necessitating frequent recalibration to account for variations in SMR patterns over time (Wolpaw & Wolpaw, 2012). These differing approaches influence the design and application of SMR-based BCIs across various use cases:

- **Cursor Movement in One or More Dimensions:** Early SMR-based BCI systems demonstrated the ability to control cursor movement on a computer screen by modulating the μ rhythm amplitude through MI. Users typically began by imagining specific limb movements, which altered SMR activity recorded over sensorimotor regions. With practice and adaptive feedback, control often became more intuitive and less dependent on conscious imagery. While this application was foundational in the development of BCI systems, it is now largely considered obsolete due to the emergence of more efficient and user-friendly paradigms for cursor control (Wolpaw et al., 1991).

- **Communication Interfaces:** SMR-based BCIs have also been utilized to support communication in individuals with severe motor impairments, such as those with amyotrophic lateral sclerosis. In such systems, imagined movements were used to select characters or words from on-screen menus, enabling basic text generation. However, this approach has been

superseded by more advanced paradigms that offer improved accuracy, speed, and usability (Kübler et al., 2005).

- **Robotic Limb Control**: SMR-based BCIs have been successfully employed in the control of robotic limbs, enabling individuals with paralysis or limb loss to perform functional tasks. For instance, Pfurtscheller et al. developed an orthotic device that allowed users to open and close a paralyzed hand through MI. By imagining movements of the impaired or missing limb, users generate specific SMR modulations, which the BCI translates into control signals for prosthetic or robotic devices. This application significantly enhances user autonomy and quality of life by enabling basic daily tasks such as eating or object manipulation (Pfurtscheller et al., 2000).

- **VR and Gaming:** SMR-based BCIs are increasingly integrated into virtual environments and gaming applications, which offer a promising combination of rehabilitation and entertainment. These systems allow users to navigate virtual worlds or control avatars through MI, with the BCI interpreting SMR variations to enable interaction. Such applications provide a safe and cost-effective platform for testing BCI systems in complex scenarios that might be impractical or dangerous in real life. Additionally, they offer therapeutic value by engaging users in motivating activities, contributing to cognitive and emotional well-being (Coogan & He, 2018).

- **Neurorehabilitation:** MI has become a central component in SMR-based BCI systems aimed at neurorehabilitation. These systems decode user intent based on SMR fluctuations in EEG signals and provide real-time feedback to reinforce correct imagery patterns. This feedback loop supports the enhancement of the central nervous system's natural output. SMR-based BCIs have shown promise in rehabilitation protocols for stroke survivors and individuals with spinal cord injuries, contributing to the recovery of motor function and overall improvements in life quality (Cantillo-Negrete et al., 2023; Yuan & He, 2014).

2.1.6.1 LOWER LIMB EXOSKELETON CONTROL

BCIs represent a rapidly evolving technology that enables direct communication between the brain and external devices, bypassing traditional neuromuscular pathways. This innovation holds significant promise for individuals with motor impairments, particularly those resulting from spinal cord injury, stroke, or limb amputation. Among the most impactful applications of BCIs is the control of prosthetic devices, allowing users to perform goal-directed actions through the decoding of neural activity. This can be achieved translating brain signals, typically recorded through non-invasive methods such as EEG, into control commands. Hence, BCIs offer the potential for intuitive, real-time interaction with artificial limbs and assistive robotic systems (Wolpaw & Wolpaw, 2012). Historically, BCI research has primarily focused on upper-limb prostheses. These systems have demonstrated considerable progress in decoding motor intentions to control robotic arms or hand prostheses, with applications ranging from basic grasping to complex multi-joint movements (Lebedev & Nicolelis, 2006). In contrast, lower-limb prosthetic control via BCIs remains relatively underexplored. This disparity is partly due to the increased biomechanical and control complexity of gait, balance, and posture compared to arm movements. Furthermore, the cortical representation of lower-limb movement is less accessible and less well-characterized, posing additional challenges for reliable signal acquisition and decoding (Chaudhary et al., 2016).

Despite these limitations, lower-limb exoskeletons controlled via BCIs are emerging as a promising avenue, particularly in the field of neurorehabilitation. A key approach in this context involves the use of MI, which is the mental simulation of movement without actual execution, as a control strategy. Notably, MI has been shown to activate cortical areas like those involved in actual movement execution, making it an effective proxy for inducing neuroplastic changes (Decety, 1996; Pfurtscheller & Neuper, 2001). As a result, BCIs based on MI not only provides a control mechanism for assistive devices but also stimulates cortical reorganization and functional recovery, offering dual benefits in terms of mobility assistance and rehabilitation (Lotte et al., 2013; Ramos-

Murguialday et al., 2013). Nevertheless, implementing BCI-driven control in lower-limb systems is far from trivial. EEG signals are prone to noise and variability, and gait-related cortical signals are typically more subtle than those associated with upper-limb tasks. In addition, decoding lower-limb motor intentions in real time requires robust and adaptive algorithms capable of dealing with dynamic and non-stationary conditions. To address these challenges, recent efforts have applied DL models, such as CNNs and LSTMs to improve the accuracy and generalizability of EEG decoding. These models have demonstrated the ability to learn complex spatiotemporal patterns and adapt to inter-subject variability without extensive manual feature extraction (Belal et al., 2024). Moreover, hybrid architectures that combine EEG with other biosignals, such as EMG, are showing promise in improving robustness and responsiveness in real-world conditions (Miguel-Fernández et al., 2023).

The integration of BCI and DL-based control in lower-limb exoskeletons is a rapidly evolving field. As portable EEG systems improve and DL models become more efficient and interpretable, BCI-controlled gait assistance is expected to transition from controlled laboratory settings to practical rehabilitation environments. Ultimately, this approach holds the potential to deliver highly personalized, intention-driven therapy that not only supports locomotion but also drives cortical reorganization and long-term functional recovery (Belal et al., 2024). In alignment with these emerging trends, this project focuses specifically on the application of BCI technology for the control of a lower-limb exoskeleton. By analyzing EEG signals associated with MI and decoding intention-related activity, particularly from the sensorimotor cortex, this study aims to contribute to the advancement of BCI-assisted gait systems, while also promoting brain-driven rehabilitation in individuals with lower-limb motor impairments.

2.1.7 MOTOR IMAGERY vs MOTOR EXECUTION

MI and ME constitute essential components in the investigation of BCIs and neurorehabilitation. The interaction between these two paradigms is particularly relevant in the context of SMR-based BCIs, as both processes evoke comparable sensorimotor rhythms, although they differ in terms of amplitude and spatial distribution. Various forms of MI have been identified (Ladda et al., 2021; Yang et al., 2021):

- **Visual Motor Imagery (VMI)** refers to the mental visualization of movements and can be further subdivided based on the imagery perspective: first-person and third person (Yu et al., 2016).

    - ❖ **First-Person Perspective (Internal Visual Imagery):** This form of imagery involves envisioning the movement as if one is executing it oneself, perceiving the action through one's own eyes. For example, when imagining lifting an arm, the individual would perceive the movement from a personal, egocentric viewpoint. First-person VMI predominantly activates the motor cortex, premotor areas, and the SMA, indicating a substantial overlap with the neural mechanisms engaged during actual movement execution.

    - ❖ **Third-Person Perspective (External Visual Imagery):** In this case, individuals mentally simulate observing themselves performing the movement from an external standpoint, like watching a video recording of their own actions. For instance, they might visualize their entire body completing a task as if viewed from a distance. Third-person VMI elicits activity not only in motor-related regions but also in visual processing areas such as the occipital cortex. This more extensive activation pattern reflects the engagement of visuospatial processing and dynamic movement observation.

- **Kinesthetic Motor Imagery (KMI)** emphasizes the internal bodily sensations associated with movement, such as muscle tension, joint positioning, and spatial orientation. In contrast to

visual imagery, which involves the mental visualization of movement, KMI is centered on the subjective experience of feeling the movement. For example, when imagining lifting a weight, an individual concentrates on the perceived muscle contraction and the resistance of the weight. KMI is known to activate the somatosensory cortex, which processes bodily (Ridderinkhof & Brass, 2015) motor cortex (Ridderinkhof & Brass, 2015).

2.1.8 DEEP-LEARNING

DL represents a specialized branch within AI and ML that leverages multi-layered neural networks, commonly known as deep neural networks, to identify and learn intricate structures in extensive datasets. AI broadly refers to a collection of computational approaches aimed at emulating human cognitive abilities such as learning, reasoning, and adaptive decision-making, typically through structured algorithms (Ávila-Tomás et al., 2021). In recent years, interest in AI has surged, capturing the attention of both researchers and the public. This discipline is considered part of the wider data science field, which also includes conventional programming and algorithmic techniques from machine learning (Choi et al., 2020).

DL, a distinct approach within machine learning, enables systems to progressively enhance their performance through the accumulation of data and experience. This technique excels at modeling real-world phenomena by constructing computational representations that build hierarchical structures where complex concepts emerge from simpler ones. Unlike traditional models, DL frameworks integrate feature extraction and classification into a unified, end-to-end process. This integration allows the model to automatically refine relevant features during training, reducing the dependence on extensive domain-specific expertise for manual feature engineering (Alzubaidi et al., 2021).

2.1.8.1 NEURAL NETWORKS FOR EEG DECODING

One of the primary challenges faced by BCIs is achieving reliable EEG signal decoding. Traditional ML techniques often depend on calibration sessions tailored to each subject and recording instance, largely due to variability between individuals and recording sessions (Saha & Baumert, 2020). In contrast, DL models have demonstrated enhanced performance in this regard, benefiting from their ability to incorporate transfer learning, which helps generalize across subjects and sessions. Several studies have demonstrated the effectiveness of CNNs in decoding EEG data across multiple experimental contexts (Lawhern et al., 2018; Schirrmeister et al., 2017). The most prominent CNN-based architectures developed for EEG decoding are:

- **CNN-BLSTM:** This model integrates 1D convolutional layers with two Bidirectional Long Short-Term Memory (BLSTM) layers, allowing it to extract both spatial and temporal patterns in sequential EEG data. This hybrid CNN–RNN approach is particularly effective for tasks that rely on capturing time-dependent dynamics.

- **DeepConvNet:** This architecture consists of four convolutional blocks, each followed by max-pooling, with an initial layer specifically tailored to raw EEG input. It ends with a dense softmax layer for classification. Its design enables direct decoding of task-related information from raw EEG without the need for manual feature engineering.

- **EEGNet:** It uses depthwise and separable convolutions to explicitly connect spatial and temporal filtering processes. It incorporates batch normalization, dropout, and average pooling layers to improve generalization and reduce overfitting. Due to its efficiency and low computational demands, EEGNet is highly suitable for real-time applications.

- **ShallowConvNet:** This architecture prioritizes frequency-based feature extraction using fewer layers and a larger temporal convolution kernel. This design allows the model to learn the

temporal structure of band power changes within trials, making it useful for low-complexity classification problems.

- **EEG-Inception:** It is a model that integrates inception modules to facilitate multi-scale temporal feature extraction. This design enhances robustness and improves classification performance across varied EEG patterns by analyzing feature maps at different scales.

- **EEGSym:** This model includes both inception modules and residual connections to enhance spatial feature learning. A key innovation of EEGSym is the inclusion of brain symmetrical constraints by aligning its architecture with the midsagittal plane. It also employs advanced data augmentation techniques, such as patch perturbation and hemisphere perturbation, to increase training diversity. As a result, EEGSym has shown notable improvements in inter-subject binary classification tasks involving MI.

EEGSym and EEG-Inception obtained the highest metrics for inter-subject binary classification in MI tasks, demonstrating robustness, the ability to capture multi-scale features through inception modules, and effective cross-subject and cross-dataset generalization (Perez-Velasco et al., 2022). Additionally, it was shown that EEGNet is designed to generalize across multiple BCI paradigms while achieving high accuracy, even with limited training data. This architecture is grounded in well-established EEG signal processing concepts and supports both within-subject and cross-subject classification and is highly suitable for real-time applications (Lawhern et al., 2018). We selected these three DL architectures for testing in this MSc Thesis.

2.1.8.2 EVALUATION METRICS FOR DEEP-LEARNING MODELS

To assess the performance of the DL architectures implemented in this MSc Thesis, a comprehensive set of evaluation metrics was applied. These metrics were selected for their ability to quantify not only statistical performance, but also the functional reliability of the models in the context of BCI applications. The following metrics were used:

- **Accuracy:** The overall proportion of correctly classified samples, defined as the number of true positives and true negatives divided by the total number of predictions.

- **Precision:** The proportion of positive predictions that are correct. It is calculated as TP / (TP + FP), where TP is true positives and FP is false positives. In this context, precision reflects how often the model is correct when it predicts a class, thus, a key indicator for avoiding false system activations.

- **Recall:** The proportion of actual positive cases correctly identified, computed as TP / (TP + FN), where FN is false negatives. High recall indicates that the model detects a class reliably when it is truly present, an essential feature for system responsiveness.

- **F1-Score:** The harmonic mean of precision and recall: 2 × (Precision × Recall) / (Precision + Recall). This metric balances the trade-off between missed detections (false negatives) and false activations (false positives). It is particularly important when both types of error impact usability and safety.

- **False Positive Rate (FPR):**

  - FPR for class 0 (rest) = FP / (FP + TN), indicating how often rest trials were incorrectly classified as MI. This is crucial in assessing the model's safety, as false positives in this class lead to unintended actions.

  - FPR for class 1 (MI) = FN / (FN + TP), which measures the failure to detect actual user intent—affecting system responsiveness.

- **True Positive Rate (TPR) and True Negative Rate (TNR):** These provide class-specific insight into correct predictions. TPR is equivalent to recall for the MI class, while TNR = TN / (TN + FP), assessing how well the model suppresses false activations during rest.

- **Confusion Matrix:** In addition to scalar metrics, a confusion matrix was computed for each model. This is a 2×2 table summarizing the number of:

    - **True Positives (TP):** MI trials correctly classified as MI
    - **False Positives (FP):** Rest trials misclassified as MI
    - **False Negatives (FN):** MI trials misclassified as Rest
    - **True Negatives (TN):** Rest trials correctly classified as Rest

The confusion matrix provides immediate insight into class-specific error patterns. For example, a model with high TP and FP may appear to perform well in recall but would generate many false activations, an unacceptable behavior in a real-time BCI system. An ideal matrix would maximize TP and TN while minimizing FP and FN.

3 MATERIALS AND METHODS

3.1 PARTICIPANTS

A single participant was included in this study: a 23-year-old male with no previous experience in EEG or MI tasks. Focusing on a single subject allowed for tighter control over experimental conditions, including consistent electrode placement, minimal signal variability, and stable interaction with the exoskeleton hardware. This was particularly important given that the goal of the study was not to assess inter-subject generalizability, but rather to examine the feasibility and technical integration of DL models capable of decoding motor imagery-related EEG patterns in real time for a lower limb exoskeleton control. Moreover, EEG-based BCIs are inherently sensitive to individual differences in cortical anatomy, brain rhythms, and cognitive strategies. Training DL models on data from a single participant facilitated the adaptation of the system to that subject's unique neural signature and cognitive physiology.

3.2 EXPERIMENTAL PARADIGM

In the experimental protocol we designed, the subject performed various MI tasks while his brain activity was recorded using a Bitbrain Versatile 8-channel EEG system (Versatile Water-based EEG cap, 2025), SENNSLITE® (Sensslite, 2025) and MEDUSA© software (Santamaría-Vázquez et al., 2023). The experiment consisted of two distinct tasks focusing on resting and imagined movements.

- **Motor Imagery of both feet:** A visual target appeared on the screen indicating the movement of the feet. Subject imagined the movement of their feet until the target disappeared.

- **Resting state:** A visual target appeared on the screen indicating to rest. Subject relaxed until the target disappeared.

The subject recorded 1100 trials in a total of 44 different runs, performing 25 trials per run.

From the total, 550 trials corresponded to MI of the feet and 550 trials for resting state. The Run structure, which contains the temporal organization of a complete BCI recording session, is shown in Figure 11 and is composed of the following sequential phases:

1. **Calibration Phase (0–6 s):** This initial segment is used to calibrate the system. This step ensures that subsequent decoding or classification is accurate and individualized.
2. **Pre-run Phase (6–7 s):** A short transitional period used to prepare the participant and the system for the sequence of trials.
3. **Trial Block (7–25 s):** This section contains a series of 10 trials.
4. **Post-run Phase (25–27 s):** After all trials are completed, this final phase allows participant rest.

The trial structure is also shown in Figure 11, with a total duration of 12 seconds for each trial and is divided into four distinct phases, each with a specific function in the experimental protocol:

1. **Preparation Phase (0–3 s):** This phase begins with an alert sound around 0.5 s, followed by a cue sound at 2 s, which indicates the upcoming MI task. The interval between these two auditory cues defines the update window, during which the subject prepares mentally for the task. No motor activity is required during this stage.

2. **Motor Imagery Phase (3–8 s):** Starting immediately after the cue, the subject engages in MI feet movement without actual execution. In this experiment, no real-time feedback was provided.

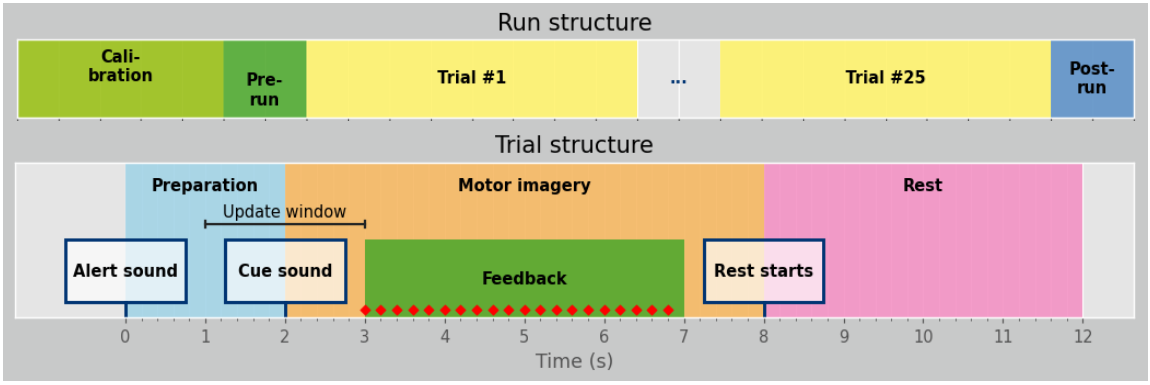

Figure 11. Run and trial structures of the experimental paradigm.

3. **Rest Phase (8–12 s):** A rest cue appears at the 8-second mark, signaling the subject to return to a relaxed state. This recovery period is essential to reset neural activity before the next trial.

3.3 SIGNAL ACQUISITION

EEG data were acquired using the Bitbrain Versatile EEG cap, a mobile, water-based EEG system available in configurations of 8, 16, 32, or 64 channels. For this study, a version with 8 electrodes was used, with sensors positioned according to the international 10/20 system [F3, C3, P3, Cz, Pz, F4, C4, P4]. EEG signals were recorded at a sampling rate of 256 Hz and transmitted wirelessly via Bluetooth to an HP Pavilion x 360 laptop. For data acquisition SENNSLITE® software was employed. This software provides millisecond-level synchronization with the Versatile EEG cap and supports integration with third-party software through the Lab Streaming Layer (LSL). The LSL protocol is an open-source framework specifically designed to facilitate real-time synchronization and the seamless exchange of time-series data across multiple hardware and software components, particularly in the fields of neuroscience and experimental psychology. Its primary function is to streamline the integration of data in multimodal experimental setups, ensuring that signals acquired from heterogeneous sources are temporally and contextually aligned with high precision. This protocol facilitated seamless and precise synchronization, allowing real-time data visualization using MEDUSA© software and subsequent analysis using Python. The complete pipeline of the signal acquisition process is shown in Figure 12.

3.3.1 MEDUSA© SOFTWARE

MEDUSA© is a versatile, open-source platform for modern non-invasive BCI applications, developed by the Biomedical Engineering Group at the Universidad de Valladolid (Santamaría-Vázquez et al., 2023). Its core functionalities include: (1) extensive compatibility with a wide range of signal acquisition systems, enabled by the LSL protocol for the synchronized recording of multiple signals; (2) a rich suite of BCI paradigms and cognitive neuroscience experiments,

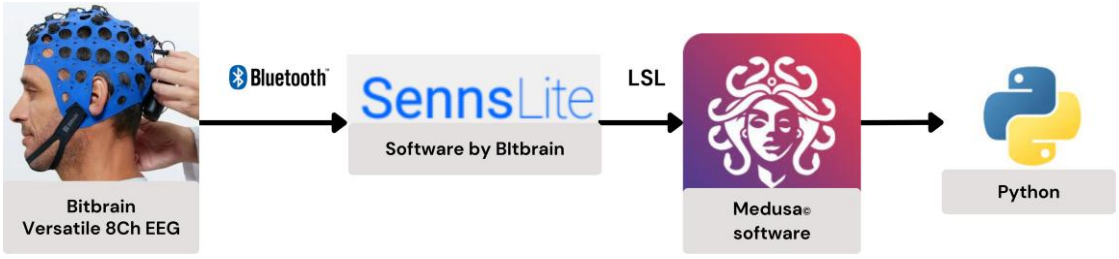

Figure 12. Pipeline of the signal acquisition process.

encompassing ERP-based spellers, MI, neurofeedback, and neuropsychological tasks; (3) advanced signal processing techniques for both offline and online analysis, including deep learning and connectivity metrics; (4) developer-friendly tools for creating custom open- and closed-loop experiments; and (5) dedicated features promoting open science, reproducibility, and community collaboration, such as an integrated app marketplace and interactive discussion forums. The platform consists of two distinct components:

- **MEDUSA© Kernel**: A Python package that provides a comprehensive set of tools for brain signal analysis. It includes state-of-the-art techniques in signal processing, machine learning, deep learning, and high-level analytics. Additionally, it supports various biosignals types (e.g., EEG, MEG) and offers functionalities for data storage and the development of standalone processing pipelines.
- **MEDUSA© Platform**: A Python-based desktop application offering high-level experimental control through a modern graphical user interface. It features advanced signal acquisition capabilities and real-time visualization. A key feature is its modular architecture, which allows users to install and develop applications for conducting neuroscience and BCI experiments, all powered by the underlying MEDUSA© Kernel for real-time signal processing.

Among the numerous modules available in the MEDUSA© Kernel, ranging from artifact removal to spatial and temporal filtering, those specifically dedicated to MI are of relevance to our study. These modules offer robust classification pipelines suitable for both offline and online use, visualization tools for MI-specific analysis, and optimized data structures tailored to MI decoding tasks.

3.3.2 SENNSLITE® SOFTWARE

SENNSLITE® is software developed by Bitbrain for the real-time acquisition and visualization of neurophysiological signals. This application is part of Bitbrain's neurotechnology ecosystem and is specifically designed to integrate seamlessly with its EEG systems, such as the Versatile 8 ch EEG device used in this MSc Thesis. In this study, SENNSLITE® served as the primary platform for data acquisition during participant training sessions. The software enables live visualization of EEG signals across multiple channels and provides key monitoring tools such as impedance checking, electrode quality feedback, and event synchronization. SENNSLITE® supports the LSL protocol, which ensures precise time synchronization of EEG signals with external stimuli or events. This feature allowed the recorded data to be streamed in real time to other processing environments such as MEDUSA©, for subsequent analysis and storage. The software also features a user-friendly interface for configuring key acquisition parameters, including sampling rate, active channel selection, hardware filters, and session protocols. This flexibility makes it suitable for both clinical and research applications in BCI development.

3.4 DATASETS

To conduct our study, we surveyed publicly available databases involving healthy subjects engaged in MI tasks. After exploring multiple repositories, we selected the EEG Motor Movement/Imagery Dataset v1.0.0 available on PhysioNet. This dataset was chosen primarily due to its relatively large cohort size (109 subjects) compared to other publicly available alternatives. PhysioNet is a well-established and comprehensive repository of physiological and clinical data, maintained by the MIT Laboratory for Computational Physiology. It provides open access to extensive collections of recorded physiological signals and associated open-source software. It has become a vital resource for the scientific community, facilitating the development and evaluation of advanced algorithms and analytical tools for complex physiological signal processing (Goldberger et al., 2000; Schalk et al., 2022, 2004).

In addition to the PhysioNet dataset, we incorporated the AlexMI dataset, accessible through the MOABB (Mother of All BCI Benchmarks) framework. This dataset comprises MI-EEG recordings from eight healthy participants from the PhD dissertation of A. Barachant (Barachant,

2012). The inclusion of this dataset, despite its smaller sample size, provides a valuable contrast in terms of experimental design and recording parameters, thereby enriching the diversity and robustness of our analysis

3.4.1 EEG MOTOR IMAGERY DATASET PHYSIONET BCI2000

Due to the limited availability of public EEG datasets implementing a MI feet vs resting paradigm, we opted to use the PhysioNet BCI2000 dataset as a pre-training source for our DL models. Although this dataset does not include a direct comparison between foot-related MI and true resting-state activity, it offers labeled trials for both ME and MI tasks involving the fists and the feet, which can be repurposed to approximate the desired classification paradigm. To adapt the dataset to our study objectives, all trials involving foot-related activity, whether imagined or executed were grouped and labeled as Feet MI. In contrast, all hand-related trials, whether imagined or executed were used to represent the Resting State class. This binary classification setup allows the models to learn discriminative neural patterns associated with lower-limb motor imagery by contrasting them against a controlled baseline of upper-limb activity. This strategy was employed to initialize the models with relevant neural representations prior to training them on subject-specific data in the BCI paradigm. The goal was to guide the models toward extracting invariant features, such as SMRs, and to improve their ability to generalize real-time MI decoding tasks tailored to the control of a lower-limb exoskeleton.

The dataset was developed by Gerwin Schalk and collaborators at the BCI R&D Program, Wadsworth Center, New York State Department of Health, Albany, NY. It was produced by the creators of BCI2000, an open-source and highly flexible software platform designed to support BCI research and development. BCI2000 offers an integrated framework for real-time data acquisition, signal processing, and the presentation of stimuli and feedback. It is widely recognized as a valuable tool in the field, compatible with a broad range of data acquisition systems and applicable to diverse BCI domains, including neurorehabilitation, assistive communication, and control systems (Schalk et al., 2022). Specifically, the dataset used in our study was released in 2009 and comprises 64-channel EEG recordings collected from subjects performing a range of motor execution and MI tasks as part of brain-computer interface research. The dataset includes more than 1,500 EEG recordings, each lasting one to two minutes, from a total of 109 participants. However, no sociodemographic information about the subjects is provided (Schalk et al., 2004).

The experimental protocol involved participants performing a series of motor execution and MI tasks while their brain activity was recorded using a 64-channel EEG system and the BCI2000 software platform. The experiment included baseline measurements as well as four distinct task conditions, encompassing both actual and imagined motor activities (Schalk et al., 2022). The baseline phase comprised two separate one-minute runs: one with the participants' eyes closed and another with their eyes open. Regarding the four task conditions, each was designed to engage different motor and cognitive processes:

1. **Motor Execution of One Hand**: A visual target appeared on either the left or right side of a screen. Participants were instructed to repeatedly open and close the corresponding fist for the duration of the stimulus and then return to a relaxed state once the target disappeared.
2. **Motor Imagery of One Hand**: Identical to the previous task in visual presentation, participants instead imagined performing the corresponding fist movement, without actual muscle activation, until the target vanished.
3. **Motor Execution of Both Fists or Feet**: A visual target appeared either at the top or bottom of the screen. If the cue was presented at the top, participants executed repeated bilateral fist movements; if at the bottom, they moved both feet. Upon the target offset, they returned to rest.
4. **Motor Imagery of Both Fists or Feet**: This task followed the same visual cueing structure as Task 3. However, participants were instructed to imagine the movement (either fists or feet) rather than physically performing it.

The experimental session began with two one-minute baseline recordings: one with the subject's eyes open and another with eyes closed. Following these, each of the four tasks was performed in a fixed order across three repetitions:

1. **Baseline:** eyes open
2. **Baseline:** eyes closed
3. **Task 1:** Left or right fist movement
4. **Task 2:** Left or right fist imagined movement
5. **Task 3:** Bilateral fists or feet movement
6. **Task 4:** Bilateral fists or feet imagined movement

This sequence was repeated three times, resulting in a total of 14 experimental runs. The collected EEG data were stored in EDF+ format, with accompanying annotation files for each recording. These annotation files contain event markers corresponding to specific phases of the trials:

- **T0**: Denotes rest periods.
- **T1**: Marks the onset of motion involving:
    - The left fist in runs 3, 4, 7, 8, 11, and 12
    - Both fists in runs 5, 6, 9, 10, 13, and 14
- **T2**: Marks the onset of motion involving:
    - The right fist in runs 3, 4, 7, 8, 11, and 12
    - Both feet in runs 5, 6, 9, 10, 13, and 14

3.4.2 EEG MOTOR IMAGERY DATASET ALEXMI

The AlexMI dataset originates from a PhD dissertation and is available through the MOABB framework. It contains EEG recordings from eight healthy participants, each performing three MI tasks: right-hand movement, feet movement, and rest. Recordings were conducted using a g.USBamp EEG amplifier with a 512 Hz sampling rate and 16 wet electrodes positioned according to the international 10–20 system: Fpz, F7, F3, Fz, F4, F8, T7, C3, Cz, C4, T8, P7, P3, Pz, P4, and P8 (Barachant, 2012).

The recordings are provided in MNE raw file format, with an associated stimulation channel that encodes the trial structure. Each trial begins with a marker "1" for trial start, followed by: "2" for right-hand MI, "3" for feet MI, and "4" for rest. Each trial lasts 3 seconds, with 20 trials per class per subject. For the purposes of this study, only trials corresponding to feet MI and rest were used. All trials involving right-hand MI were discarded. The selected trials were relabeled into two categories: *Feet MI* as the target class and *Resting State* as the baseline class. This configuration was chosen to pre-train DL models to distinguish neural patterns specifically related to lower-limb MI, eliminating potential interference from upper-limb activity. This selection strategy contributes to the development of robust pretraining pipelines, enabling models to better generalize when decoding lower-limb MI tasks in more complex or subject-specific contexts.

3.5 EEG PREPROCESSING

The raw EEG signals from the recordings and datasets underwent a series of preprocessing steps to ensure consistency and suitability for deep learning-based classification (Perez-Velasco et al., 2022).

1. **Extraction of channels:** A subset of channels was selected according to one standard configuration: an 8-channel setup comprising 'F3', C3', P3', Cz', Pz', F4', C4', and 'P4',

following the international 10/20 electrode placement system. These configurations are commonly adopted in low-cost EEG caps due to their balance between spatial coverage and minimal setup time.

2. **Application of a fourth-order infinite impulse response (IIR) notch filter:** to remove power line interference at 50 or 60 Hz, depending on the dataset, particularly in cases where this artifact had not been removed through hardware means.

3. **Application of a common average reference (CAR) spatial filter**: across the selected channels to enhance the signal-to-noise ratio by minimizing spatially correlated noise.

4. **Resampling:** all the signals to 128 Hz to standardize the temporal resolution across datasets.

5. **Extraction of trials:** using a fixed time window of 3 seconds post-stimulus onset, which represented the maximum duration uniformly available across all datasets without requiring signal padding or discarding incomplete trials.

6. **Application to each trial of a channel-wise z-score standardization:** transforming each channel to have zero mean and unit variance. This step eliminates any direct current (DC) component and scales the data appropriately for input into a deep learning model.

3.6 CLASSIFICATION AND TRANSFER LEARNING

As previously discussed, the DL models selected for this study are EEGNet, EEG-Inception, and EEGSym, due to their proven performance in EEG-based MI classification tasks. In the present work, a pretraining strategy was applied using the external datasets PhysioNet BCI2000 and AlexMI, to allow the models to learn generalizable patterns associated with MI. Following this, a fine-tuning phase was conducted using the subject-specific recordings acquired during the experimental sessions. This two-stage training process aims to leverage both inter-subject variability and individual specificity to enhance model robustness and accuracy. The methodology associated with each phase is detailed in the subsequent sections.

3.6.1 EEGNet

EGNet is a compact convolutional neural network architecture proposed by (Lawhern et al., 2018) designed specifically for EEG-based BCI applications. The architecture was developed with the goals of interpretability, generalizability across paradigms, and efficient training with limited data. Unlike traditional deep models adapted from computer vision, EEGNet incorporates architectural elements explicitly aligned with conventional EEG signal processing techniques, such as bandpass filtering and spatial filtering. This makes EEGNet particularly well-suited for BCI paradigms involving MI, P300, and SSVEP. This architecture achieves these goals by using depthwise and separable convolutions, which drastically reduce the number of trainable parameters while preserving its ability to learn spatio-temporal features. This parameter-efficient design allows EEGNet to perform well even when training data is scarce, a common scenario in BCI research. The architecture can be divided into three main blocks, which are illustrated in Figure 13:

- **Temporal and Spatial Filtering:** The first layer applies a 2D convolution with filters of size (1 × 64), which operate over the temporal domain and simulates bandpass filtering. This is followed by a depthwise convolution, where spatial filters are learned for each temporal filter independently. This mimics spatial filtering operations such as CSP. These layers are followed by batch normalization, an ELU activation, average pooling, and dropout, which together enhance model stability and reduce overfitting.

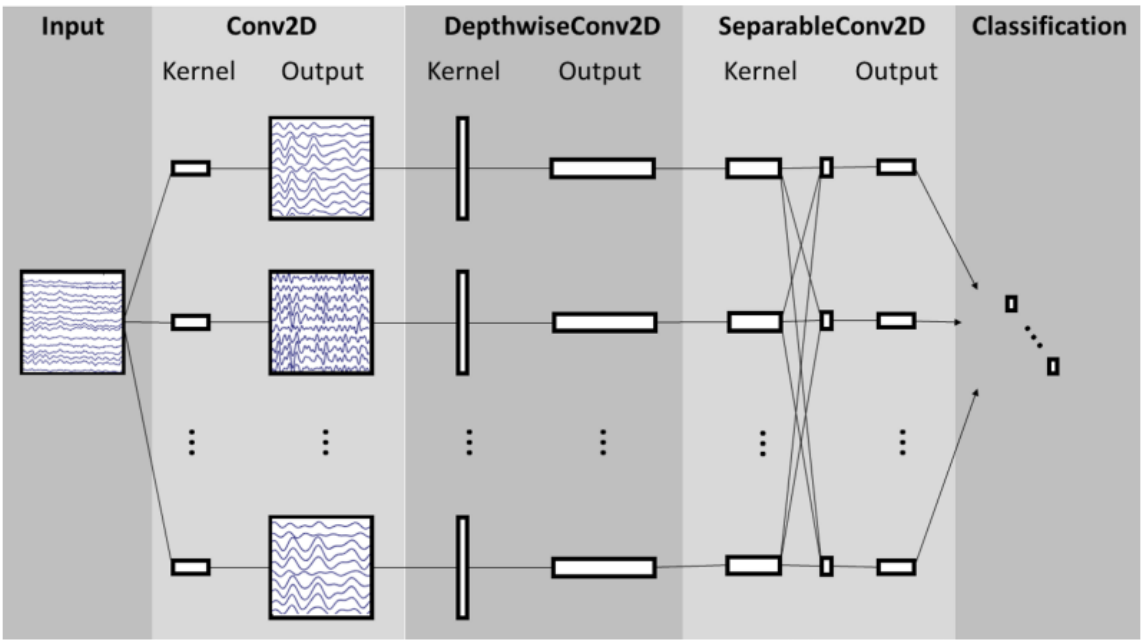

Figure 13. Overall visualization of the EEGNet architecture. Lines denote the convolutional kernel connectivity between inputs and outputs (called feature maps). The network starts with a temporal convolution (second column) to learn frequency filters, then uses a depthwise convolution (middle column), connected to each feature map individually, to learn frequency-specific spatial filters. The separable convolution (fourth column) is a combination of a depthwise convolution, which learns a temporal summary for each feature map individually, followed by a pointwise convolution, which learns how to optimally mix the feature maps together (Lawhern et al., 2018).

- **Feature Aggregation:** In the second block, a separable convolution is applied to extract higher-order temporal features while reducing dimensionality. This is implemented by combining a depthwise convolution (independent filtering per channel) with a pointwise convolution (1 × 1), effectively merging spatially filtered outputs. As in the previous block, this is followed by batch normalization, ELU activation, average pooling, and dropout.

- **Output Block:** Finally, the resulting feature maps are flattened and passed through a fully connected dense layer followed by a SoftMax activation function for classification. The architecture typically outputs two or more class probabilities depending on the task.

This modular design enables EEGNet to function as a general-purpose architecture across different BCI paradigms. Moreover, each layer corresponds to a conceptually interpretable operation: temporal filtering, spatial filtering, and temporal summarization.

3.6.2 EEGInception

EEG-Inception is a CNN architecture introduced by (Santamaría-Vázquez et al., 2020), originally inspired by deep learning models developed for image classification and subsequently adapted for EEG signal analysis and ERP detection. The architecture integrates principles from computer vision, notably the use of Inception modules, which enable the extraction of features across multiple temporal and spatial scales. Additionally, it employs depthwise convolutions to enhance computational efficiency and reduce the number of parameters. Designed with a strong emphasis on preventing overfitting, EEG-Inception includes an output block that consolidates the information processed by the Inception modules into a compact representation of high-level features. Only 24 features are passed to the final classification layer, a design choice that enhances

generalization and makes the model particularly well-suited for subject-specific fine-tuning. This compact representation allows the architecture to achieve high performance with a minimal number of calibration trials, thereby facilitating efficient adaptation to new users and reducing the burden of data collection. The EEG-Inception architecture, represented in Figure 14, is composed of two sequential Inception modules, each designed to extract temporal and spatial features at multiple scales to enhance EEG signal representation.

- **Inception Module 1:** Processes the EEG signals at three distinct temporal resolutions through parallel convolutional blocks: C1, C2, and C3, which use kernel sizes of 64 × 1, 32 × 1, and 16 × 1, respectively. Given the input sampling rate of 128 Hz, these kernels correspond to temporal windows of approximately 500, 250 and 125 ms. Following these layers, the blocks D1, D2, and D3 process the signal in the spatial domain using depthwise convolutions. Originally introduced in image processing to reduce model complexity by decomposing full convolutions into separate channel-wise operations, and in depthwise convolutions in this context are applied individually to each EEG channel. This enables the network to learn optimal spatial filters tailored to the specific temporal patterns extracted in the previous layers. The outputs from the three branches are then merged by the concatenation layer N1 and passed through an average pooling layer to reduce dimensionality.

- **Inception Module 2:** Mirrors the structure of the first module but operates on a higher level of abstraction. It processes the signal at 500, 250, and 125 ms. After the average pooling, the corresponding kernel sizes are reduced to 16 × 1, 8 × 1, and 4 × 1 respectively. The outputs of convolutional blocks C4, C5, and C6 are subsequently concatenated, and another average pooling layer is applied to further reduce the dimensionality. This second module is designed to refine and consolidate the temporal features learned in the previous stage, enhancing the model's capacity to generalize across varying temporal dynamics in EEG signals.

- **Output Module:** Consists of the final two convolutional layers, which are specifically designed to extract the most discriminative patterns relevant for classification. These layers progressively reduce the number of filters, thereby compressing the learned representations into a compact set of features. This strategy not only reduces the dimensionality of the feature space but also mitigates the risk of overfitting. As a result, only 24 high-level features are passed to the final classification layer, which utilizes a SoftMax activation function to compute the probability distribution over the output classes, typically representing target and non-target conditions.

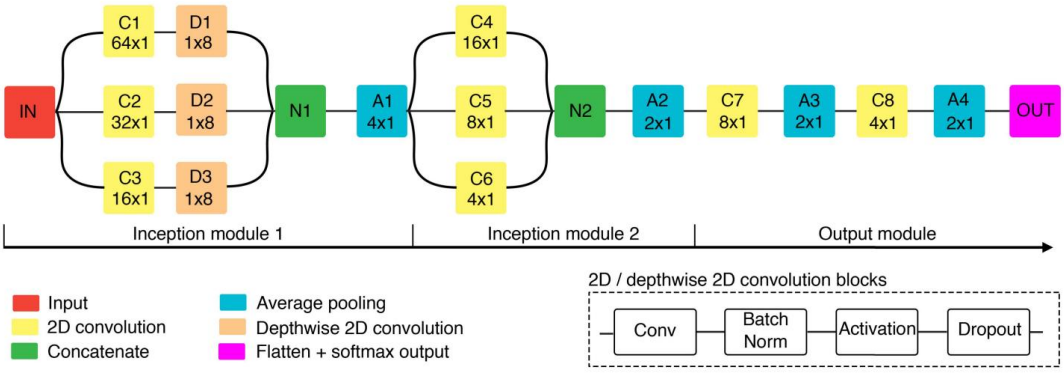

Figure 14. Overview of EEG-Inception architecture: The architecture includes both 2D convolution blocks and depthwise 2D convolution blocks, each incorporating batch normalization, activation functions, and dropout regularization. The kernel sizes for convolutional and average pooling layers are specified (Santamaría-Vázquez et al., 2020).

In the original implementation by Santamaria-Vazquez et al., the model was trained using the Adam optimizer with its default hyperparameters are $\beta_1 = 0.9$, $\beta_2 = 0.999$ and a categorical cross-entropy loss function. Training was conducted over 500 epochs with a mini-batch size of 1024. To enhance training efficiency and avoid overfitting, early stopping was employed, whereby training was halted if the validation loss failed to improve over 15 consecutive epochs. In such cases, the model weights were reverted to those that achieved the minimum validation loss. Several critical hyperparameters were automatically optimized via grid search on the validation set, including the learning rate (lr), activation function (fact), and dropout rate (dr). The optimal values identified were lr = 0.001, fact = ELU, and dr = 0.25. The remaining architectural parameters, such as the number of layers, inception branches, filters, kernel sizes, and pooling sizes, were determined heuristically. For the present study, the same training configuration was adopted with a single adjustment: due to the limited amount of available training data, the mini-batch size was reduced to 32 to ensure more stable gradient estimates during optimization.

3.6.3 EEGSym

Like EEG-Inception, the EEGSym architecture proposed by (Perez-Velasco et al., 2022), integrates several effective design strategies that have previously demonstrated strong performance in EEG decoding tasks. Notably, the model incorporates inception modules at the early stages of the network to extract multi-scale temporal features. Additionally, it employs grouped convolutions as an alternative to depthwise convolutions, emulating the structural advantages observed in both EEGNet and EEG-Inception. This approach allows the model to learn spatially specific patterns while maintaining computational efficiency. Each convolutional layer in EEGSym is systematically followed by batch normalization, exponential linear unit activation, and dropout regularization, which together enhance model stability and generalization. EEGSym's architecture, illustrated in Figure 15, unfolds across 5 stages.

Key hyperparameters were selected via grid search on the validation set, including a dr of 0.4, 24 filters in the Inception modules, and a lr of 0.001, reflecting a deliberate balance between model complexity and generalization performance.

- **Symmetric Division:** Introduces virtual subdivisions within the network, facilitating the optimization of spatial filter parameters for downstream tempospatial processing. This structural design also serves to reduce parameter redundancy, enabling more efficient learning of spatial patterns.

- **Tempospatial Analysis:** Captures complex temporal dependencies and spatial features across the EEG signal. It comprises two Inception modules and three residual blocks, with Inception kernel sizes of 64, 32, and 16, corresponding to temporal windows of 500, 250 and 125 ms, respectively mirroring the configuration used in EEG-Inception. The outputs from each convolutional operation are concatenated and integrated via residual connections, after which temporal dimensionality is reduced through average pooling. For spatial feature extraction, the architecture applies grouped convolutions across EEG channels organized by hemisphere. This reduces the number of channels to one per group while preserving the residual connections, ensuring the retention of temporal dependencies after spatial transformation. Each residual block thus performs both temporal and spatial analyses, maintaining shortcut connections throughout to preserve temporal continuity, even following spatial operations and pooling

- **Channel Merging:** Reduces the spatial dimensionality of the EEG data to a single representation across the Z and C axes by applying two convolutional layers connected via residual links. This process culminates in a grouped convolution operation, applied across hemispheres and channels using a kernel size of $2 \times 1 \times 5$, effectively integrating spatial information while preserving anatomical and functional symmetry.

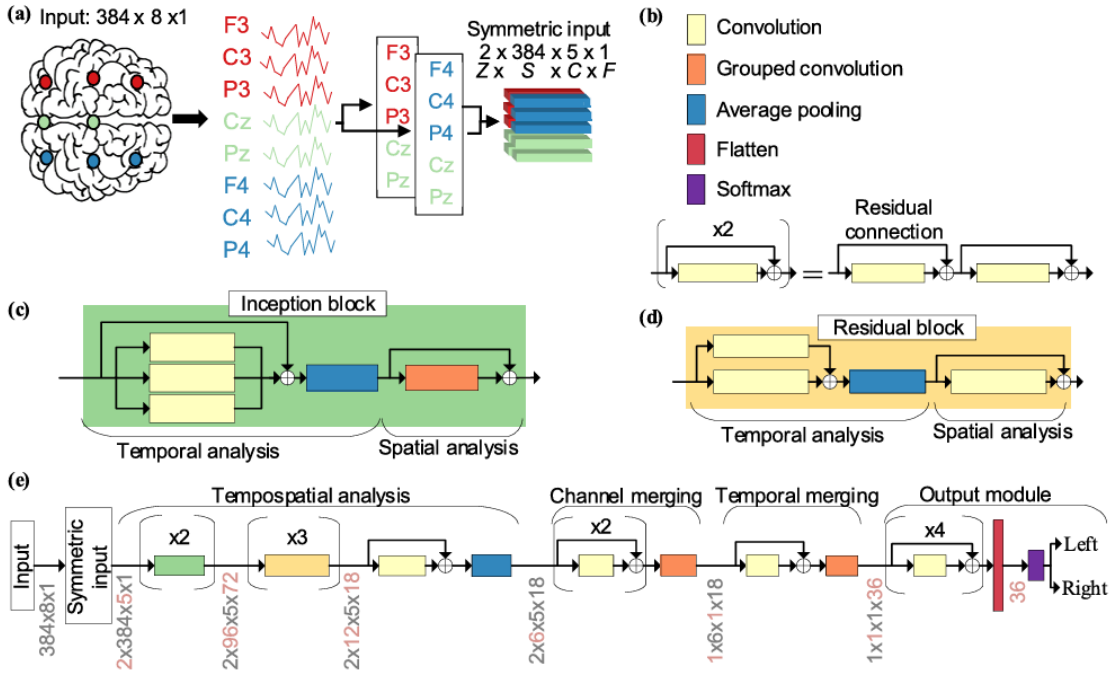

Figure 15. Overview of EEGSym architecture. (a) Schematic of the division of input electrodes for an 8-electrode configuration Z: hemispheres (i.e., 2), S: samples (i.e., 384), C: electrodes per hemisphere (i.e., 5), F: number of filters. (b) Legend of the architecture overview. (c) Inception block. (d) Residual block. (e) EEGSym architecture. All convolution and grouped convolution operations are followed by batch normalization, 'elu' activation and dropout regularization in this order. The output sizes of each operation are indicated in gray, whereas the dimension that is affected after each stage is indicated in red (Perez-Velasco et al., 2022).

- **Temporal Merging:** This stage further reduces the temporal dimensionality to a single time point S through the application of convolutional and grouped convolutional operations aligned with the temporal dimension.

- **Output Module:** The final stage produces feature representations determined by the number of filters used in the inception modules. It comprises four convolutional layers interconnected by residual connections. The resulting feature maps are subsequently flattened and passed to a SoftMax layer for classification across MI classes.

For the purposes of our study, we retain the same hyperparameter configuration as in (Perez-Velasco et al., 2022). However, in contrast to the preprocessing pipeline employed in their work, no data augmentation techniques will be applied to the input data in our experiments. This is due to the focus of this work is on evaluating model performance under realistic, subject-specific conditions, where the amount of training data is naturally limited. Applying synthetic transformations such as temporal shifts, noise injections, or spectral perturbations could introduce artificial variability that may not reflect the actual dynamics of the EEG signals acquired in our experimental setup.

3.6.4 PRE-TRAINING AND FINE-TUNING ANALYSIS

As previously mentioned, the objective of this project is to train three DL models using several datasets comprising executed and imagined movements performed by the subjects and subsequently transfer the acquired knowledge to predict imagined movements from the participant to consciously move the lower limb exoskeleton. A model-based transfer learning approach was selected as the most suitable strategy for this purpose.

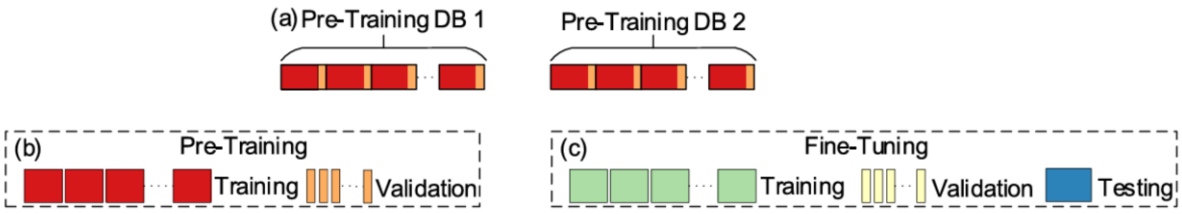

Figure 16. Pre-Training DB: datasets used for pre-training the model. Target DB: dataset in which fine-tuning and testing is performed in the participant. (a) Scheme of the pre-training datasets. (b) Pre-training dataset. (c) Fine-tuning dataset and testing subject. Image adapted from (Perez-Velasco et al., 2022).

The trials collected from the participant serve as the target dataset, on which MI prediction accuracy is evaluated. For the pre-training phase, the PhysioNet and AlexMI datasets are employed, see Figure 16. This phase produces an initialization of the model's weights, which is then used as the starting point for the subsequent fine-tuning on the target dataset. From each subject in the pre-training datasets, the data are partitioned into training and validation subsets following a 95:5 ratio. During fine-tuning, all subject trials in the target dataset except those selected for testing, shown in Figure 16, are used. The data are divided into training, validation, and testing subsets following an 80:10:10 ratio. This phase enables deeper adaptation of the feature extraction layers, which is particularly beneficial when the target dataset differs substantially from those used in the pre-training stage. This procedure is adapted from the fine-tuning recommendations provided in (Chollet, 2017).

For each model, the preprocessing steps described in subsection 3.5 were applied. The following DL techniques were implemented:

- Early stopping was used during both pre-training and fine-tuning phases, terminating the training process if the validation loss did not improve over 15 consecutive iterations.

- Pre-training was conducted on all datasets excluding the target dataset.

- A fixed learning rate of 0.01 was used for all models. This value is consistent with the open-source implementations of EEGNet provided by (Lawhern et al., 2018), with the implementation of EEG-Inception by (Santamaría-Vázquez et al., 2020) and as well with the implementation of EEGSym provided by (Perez-Velasco et al., 2022).

3.7 LOWER LIMB EXOSKELETON EXO-H3 TECHNAID

The Exo-H3, chosen to execute the output of the BCI system, is a lower-limb robotic exoskeleton developed by Technaid S.L. shown in Figure 17, designed specifically for research in human gait rehabilitation, motor control, and assistive robotics. It serves as a modular and programmable platform tailored for applications in neuroscience, physical therapy, and BCI research. The device features six degrees of freedom, with three actuated joints per leg (hip, knee, and ankle) in the sagittal plane. Each joint is powered by brushless DC motors with harmonic drive gears, enabling smooth and precise movement. The mechanical structure is composed of aerospace-grade aluminum and stainless steel, ensuring both robustness and minimal weight. The total system weight, including batteries, is approximately 17 kg. The Exo-H3 is designed to accommodate users up to 1.95 meters in height and up to 100 kg in weight (Technaid, 2025).

Its joint range of motion is suitable for physiological gait:

- Hip: –30° extension to 105° flexion
- Knee: 5° extension to 105° flexion
- Ankle: –30° dorsiflexion to 30° plantarflexion

Figure 17. Exo-H3 lower-limb robotic exoskeleton developed by Technaid S.L.

The exoskeleton integrates a comprehensive sensor suite that includes:

- 6 absolute encoders (1 per joint)
- 6 torque sensors (1 per joint)
- 4 foot pressure sensors (2 per foot)

These sensors provide high-resolution real-time feedback for joint angles, interaction torques, and gait phase recognition. Exo-H3 supports several control modes, including position and torque control. These can be adjusted in real-time, allowing researchers to implement and validate various assist-as-needed or adaptive rehabilitation strategies. Communication interfaces include CAN bus, Wi-Fi (802.11 b/g/n), and Bluetooth 3.0, enabling seamless integration with external systems, such as real-time BCI pipelines or physiological monitoring platforms. In this study we used the CAN bus to communicate with the Exo-H3. Technaid provides a real-time software environment compatible with MATLAB©/Simulink, Python, and C++, which allows the development of custom control algorithms and synchronization with external data streams. The system architecture is ROS-ready and supports integration with platforms like LSL, making it well-suited for hybrid BCI applications (Technaid, 2025).

Thanks to its flexibility and open architecture, the Exo-H3 has been widely used in scientific research focused on gait training and neurorehabilitation. It has served as a testbed for studies involving partial or adaptive assistance, and for validating intention-driven control systems using neural signals. In this project, the Exo-H3 is integrated with a real-time BCI system, where the user's mental state, classified every 3 seconds as either MI or resting, is used to toggle the exoskeleton's locomotion state. This integration demonstrates the feasibility of intention-based gait initiation using non-invasive EEG, supporting future applications in patient-specific motor rehabilitation and autonomy enhancement for individuals with mobility impairments (Supapitanon et al., 2025).

4 RESULTS AND DISCUSSION

This chapter presents the results and evaluation of the experimental evaluation and provides an in-depth discussion of the performance obtained by the three DL models developed in this thesis: EEGNet, EEGInception, and EEGSym. These architectures were implemented for the binary classification of 3 seconds of real time EEG signal into two classes: MI of both feet and resting state, as part of a broader objective to enable MI-BCI control of the EXO-H3 lower-limb exoskeleton developed by Technaid. To support this goal, a transfer learning strategy was employed. First, the models were pretrained on two public datasets PhysioNet BCI2000 and AlexMI, that contain MI EEG data from multiple subjects. The pretraining phase aimed to allow the models to learn general EEG signal features associated with motor tasks, particularly with SMR patterns generated during MI. Following pretraining, each model underwent a fine-tuning phase using a custom dataset recorded specifically for this study. This dataset consisted of 1,100 trials (550 MI, 550 Rest) obtained from a single subject performing feet MI and resting tasks using an 8-channel water-based EEG system, selected for its portability, ease of use and time efficiency in EEG cap setup. The experimental paradigm involved alternating MI of the feet and rest conditions. The EEG data were processed through a standardized pipeline including channel extraction of the 8-channel setup, notch filtering, CAR spatial filtering, resampling to 128 Hz, temporal segmentation with 3 seconds per trial, and z-score normalization per channel. Performance was evaluated using a comprehensive set of metrics: accuracy, precision, recall, F1-score, and false positive rate (FPR) for both classes. In addition, confusion matrices and training curves were generated for each model to visualize class-specific behavior and learn dynamics during fine-tuning. The following section presents the analysis of the results.

4.1 EEGNet CLASSIFICATION

EEGNet produced the strongest overall results among the three models tested, yet its performance was still far from satisfactory for deployment in a real-world BCI application. As represented in Table 1, the model achieved an accuracy of 57.89%, which is slightly above random chance in a binary classification task. While this marginal improvement is statistically real, it is not sufficient for reliable system behavior in safety-critical environments such as exoskeleton control. The precision of the model was 0.5444, indicating that just over half of the instances predicted as MI were actually MI. This reflects a relatively high level of false positives, especially problematic when the system is expected to remain inactive during rest. The recall was exceptionally high at 0.8750, meaning the model detected nearly 88% of true MI trials. This suggests that EEGNet is highly sensitive to motor imagery activity, a desirable trait in systems where responsiveness is critical, such as neurorehabilitation protocols or assisted initiation of movement. However, this strong recall came at the expense of specificity. The false positive rate for rest was 70.69%, which means that more than two-thirds of rest-state trials were incorrectly classified as MI. In practice, this would translate into frequent, unintended exoskeleton activations while the user is idle a risk in autonomous or semi-autonomous control contexts. The false positive rate for MI was only 12.50%, indicating a lower tendency to miss MI events, further reinforcing the model's bias toward predicting movement. These tendencies are confirmed by the true positive rate (TPR) for MI, which equals the recall at 0.8750, and the true negative rate (TNR) for rest, which is only 0.2931. This imbalance shows that EEGNet heavily favors classifying trials as MI, regardless of the actual underlying brain state.

Architecture	Accuracy	Precision	Recall	F1-Score	FPR Class 0	FPR Class 1
EEGNet	0.5789	0.6264	0.5841	0.5429	0.125	0.7068

Table 1. Classification metrics for EEGNet model.

The training curve in Figure 18 shows both training and validation losses decrease quickly during the first 10 epochs, indicating effective initial learning. After this point, the training loss continues to drop while the validation loss stabilizes. Importantly, the gap between training and validation accuracy remains relatively small, suggesting that the model generalizes decently on the subject-specific data. However, validation accuracy plateaus early (55–58%), which reflects an inherent ceiling in what the model can extract from the data. The curve confirms that EEGNet did not overfit, but also did not learn features strong enough to ensure reliable classification due to limited EEG input.

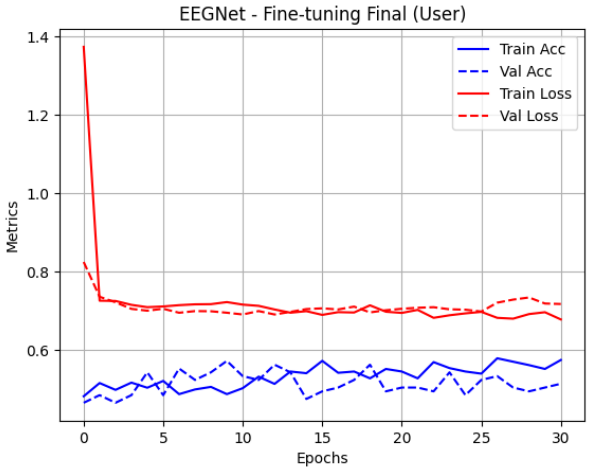

Figure 18. EEGNet Fine-Tuning Performance: Training and Validation Accuracy and Loss Curves

The matrix in Figure 19 shows that EEGNet correctly identified 49 out of 56 MI trials, which confirms the high recall (87.5%) calculated. Only 7 MI trials were identified as false negatives, which is desirable in terms of user responsiveness. However, the model misclassified 41 out of 58 resting trials as MI (false positives), while only correctly identifying 17.

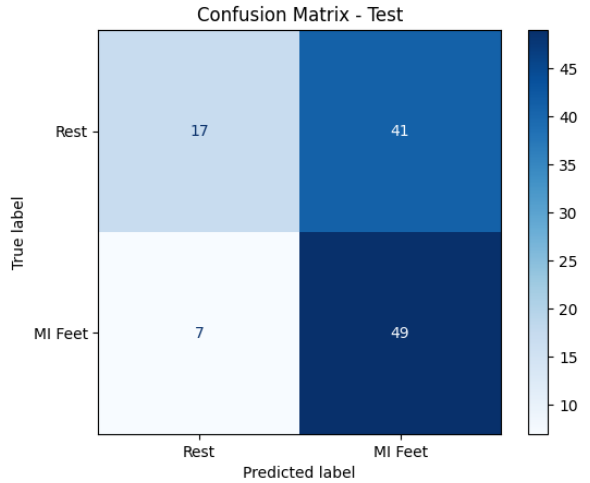

Figure 19. EEGNet Confusion Matrix on the Subject-Specific Test Set.

4.2 EEGInception CLASSIFICATION

EEGInception was the least effective model in this study, exhibiting near-random behavior across nearly all evaluation metrics, as shows Table 2. The model's accuracy was 50.00%, exactly what would be expected from random guessing in a binary task and thus offers no evidence of learned discrimination between MI and rest classes. The precision stood at 0.4937, meaning less than half of MI predictions were correct. The recall was 0.6964, which is modest in isolation but insufficient when paired with low precision. It indicates that while the model detects some MI events, it does so inconsistently and cannot be relied upon to detect user intent accurately. The false positive rate for rest was 68.97%, almost identical to EEGNet, further suggesting a tendency to overpredict MI, likely due to poor class separation. The false positive rate for MI was 0.3036, meaning nearly one-third of MI trials were incorrectly classified as rest. This poor balance is also evident in the TPR for MI, which was 0.6964, and the TNR for rest, which was 0.3103. These results indicate a model that not only fails to learn consistent signal patterns but also introduces randomness in its predictions.

Architecture	Accuracy	Precision	Recall	F1-Score	FPR Class 0	FPR Class 1
EEGInception	0.5020	0.5040	0.5034	0.4824	0.3035	0.6896

Table 2. Classification metrics for EEGInception model.

The training curve for EEGInception, represented in Figure 20, reflects rapid early convergence, with a steep decrease in training loss within the first few epochs. However, the validation loss stagnates almost immediately and remains flat throughout training. This is a critical sign that the model is failing to transfer useful knowledge to the new domain. The training accuracy rises steadily and eventually diverges from validation accuracy, suggesting overfitting to the training set. The lack of improvement in validation metrics confirms that the model is memorizing training patterns but not learning generalizable EEG features relevant to the MI vs. rest task.

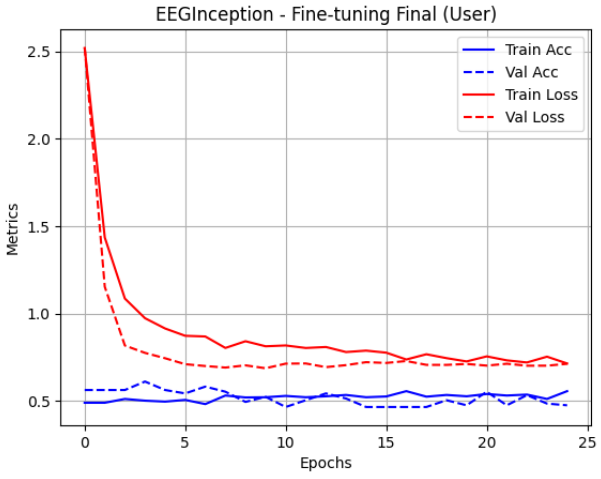

Figure 20. EEGInception Fine-Tuning Performance: Training and Validation Accuracy and Loss Curves.

The EEGInception model shows a very flat confusion matrix in Figure 21, with a high number of misclassifications in both classes. It failed to identify 17 MI trials (false negatives) and misclassified 40 resting trials as MI (false positives). Only 18 resting trials and 39 MI trials were correctly classified.

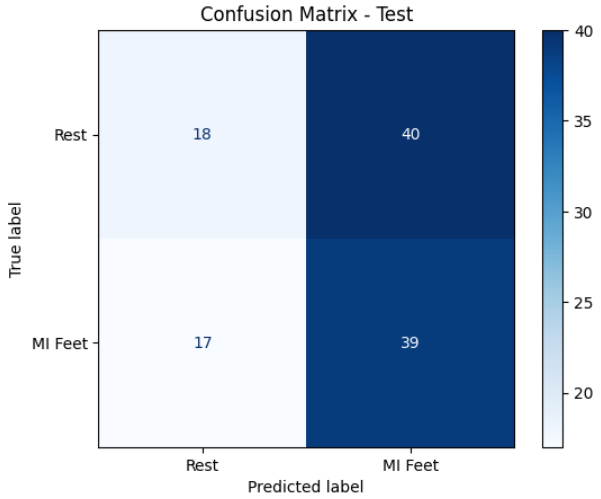

Figure 21. EEGInception Confusion Matrix on the Subject-Specific Test Set.

4.3 EEGSym CLASSIFICATION

EEGSym presented the most conservative and balanced behavior of all models tested, although its absolute performance remains insufficient for real-world use, as it is shown in Table 3. The model's accuracy was 53.51%, slightly above random chance, and its precision was 0.5246, meaning that just over half of the MI predictions were correct. Its recall was 0.5714, the lowest among the three models, indicating a higher likelihood of missing MI trials. This trade-off appears intentional: the model sacrifices some responsiveness in favor of minimizing false activations. The F1-score, combining both metrics, was 0.5470, slightly better than EEGInception but significantly below the standard required for BCI deployment. The key advantage of EEGSym lies in its false positive rate for rest, which was 0.5000, the lowest among the three models. While still too high for unsupervised use, it demonstrates a more cautious decision-making process. However, the FPR for MI was 0.4286, which is notably high and suggests the model frequently misses true MI attempts. The TPR for MI matches recall at 0.5714, and the TNR for rest was also 0.5000, showing symmetrical behavior across both classes. This is an improvement over the class bias observed in the other models, even if it comes at the cost of overall performance.

Architecture	Accuracy	Precision	Recall	F1-Score	FPR Class 0	FPR Class 1
EEGSym	0.5351	0.5359	0.5357	0.5348	0.4285	0.5000

Table 3. Classification metrics for EEGSym model.

The curve for EEGSym represented in Figure 22 shows quick stabilization of both training and validation loss, with little separation between the two, indicating good regularization and low risk of overfitting. Unlike EEGInception, EEGSym maintains a tight overlap between training and

validation accuracy across all epochs. However, the performance plateaus early, and the maximum validation accuracy remains around 53–54%, which is still close to chance. This suggests that while EEGSym is statistically stable, it lacks the representational power or signal clarity required to make strong class distinctions. The curve reflects a well-behaved model with poor input, not poor training dynamics.

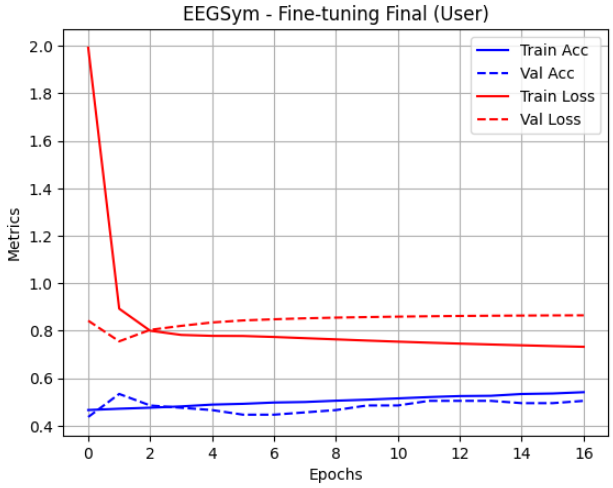

Figure 22. EEGSym Fine-Tuning Performance: Training and Validation Accuracy and Loss Curves.

This matrix in Figure 23 shows that EEGNet correctly identified 49 out of 56 MI trials, which confirms the high recall (87.5%) calculated. Only 7 MI trials were missed (false negatives), which is desirable in terms of user responsiveness. However, the model misclassified 41 out of 58 resting trials as MI (false positives), while only correctly identifying 17.

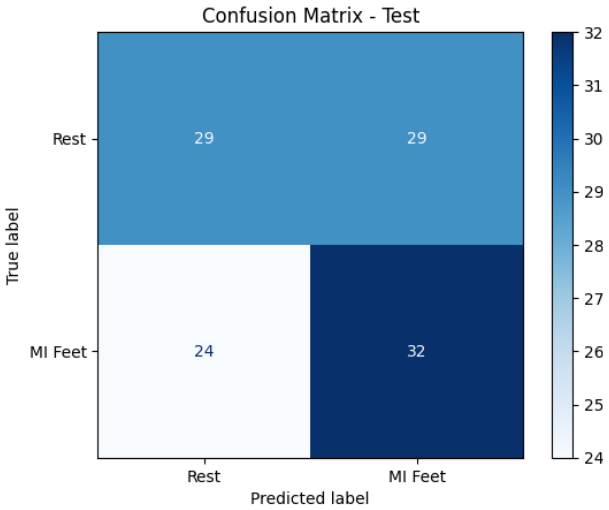

Figure 23. EEGSym Confusion Matrix on the Subject-Specific Test Set.

4.4 COMPARATIVE ANALYSIS OF THE MODELS

To better visualize the trade-offs between the models, Table 4 summarizes the performance metrics obtained by each architecture.

Architecture	Accuracy	Precision	Recall	F1-Score	FPR Class 0	FPR Class 1
EEGNet	0.5789	0.6264	0.5841	0.5429	0.125	0.7068
EEGInception	0.5020	0.5040	0.5034	0.4824	0.3035	0.6896
EEGSym	0.5351	0.5359	0.5357	0.5348	0.4285	0.5000

Table 4. Classification metrics for the three DL models.

Overall, none of the models evaluated are ready for operational use in BCI-based exoskeleton systems. The choice of architecture appears to influence class bias EEGNet toward action, EEGSym toward inhibition yet neither strikes a satisfactory compromise. These findings reinforce that the current DL paradigms, when applied in small-data, low-resolution EEG scenarios, are far from delivering robust, real-world BCI control.

4.5 REAL TIME EVALUATION WITH EXO-H3

In the final stage of the system pipeline, the real-time performance of the trained DL models is evaluated. Each of the three DL architectures: EEGNet, EEG-Inception, and EEGSym, provides a binary classification output every 3 seconds, corresponding to either a MI of the feet or resting state. These classifications are continuously updated as new EEG data segments are processed. The classification output is then used to control the Exo-H3 lower-limb exoskeleton developed by Technaid (Technaid, 2025). To enable this, a custom communication architecture was implemented. Specifically, the predictions generated in Python are transmitted in real time to MATLAB© via a socket interface. When MATLAB© receives a MI prediction, it triggers a step command by sending a structured set of parameters that control joint positions and velocities to the exoskeleton. This command initiates a predefined walking pattern in the sagittal plane, actuating the hip, knee, and ankle joints sequentially to execute one step. Conversely, when a "rest" prediction is received, MATLAB© executes a postural control command that sets all three joints on each leg to a locked position, maintaining the current posture with torque support and preventing any movement. This ensures user safety by halting locomotion and preserving balance, even in the presence of occasional misclassifications.

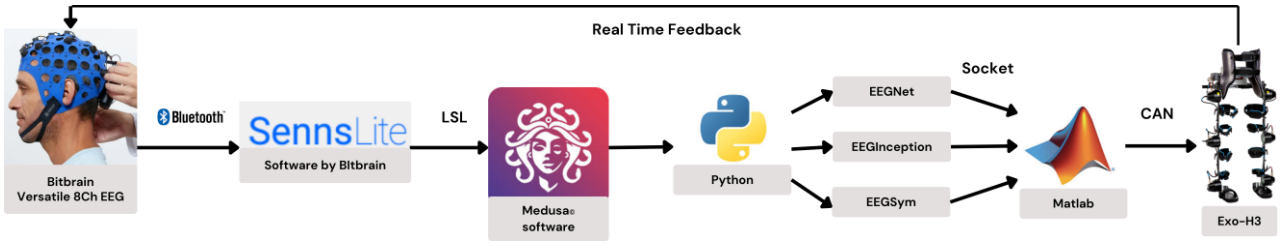

Figure 24. Pipeline of the Exo-H3 control system.

MATLAB© then serves as the intermediate control layer that interfaces with the Exo-H3 through the CAN (Controller Area Network) bus, a robust real-time communication protocol widely used in embedded systems and robotics to exchange messages between microcontrollers and devices. The CAN protocol ensures reliable transmission of low-level control commands to the exoskeleton's actuators. This modular setup allows seamless integration between the EEG decoding and the actuation of the robotic device. As a result, the system translates brain activity detected and decoded through EEG into executable commands that activate or deactivate the exoskeleton's movement mode. This setup, shown in Figure 24, enables a closed-loop BCI, where EEG-based mental commands are used in real time to initiate or inhibit robotic movement. The system has been designed to be responsive and adaptive, offering intuitive control based on the participant's mental state without requiring physical effort. This is particularly relevant in rehabilitation contexts where patients may lack voluntary control over their lower limbs.

4.6 LIMITATIONS

The performance outcomes can be traced back to several interrelated limitations, which are outlined below:

- **General Data Scarcity:** The most impactful limitation was the overall lack of training data. Deep learning architectures require large, diverse, and well-labeled datasets to learn complex spatiotemporal patterns from noisy EEG signals. In this project, the limited size of both pretraining datasets and the subject-specific recordings constrained model learning at all stages.

- **Task Mismatch in PhysioNet Dataset:** The PhysioNet BCI2000 dataset was originally designed for classifying hand and foot movements. To adapt it for MI vs. rest classification, all hand trials were labeled as "rest." However, MI of the hands is not equivalent to resting EEG, leading to feature-label inconsistency and suboptimal pretraining.

- **Small Scale of the AlexMI Dataset:** While task-aligned, AlexMI is limited in size (eight subjects with 20 trials per class). Its small scale reduced its effectiveness as a meaningful pretraining set, particularly for generalizing across cognitive states.

- **Limited Fine-Tuning Dataset:** Only one participant contributed to the subject-specific dataset. Although relatively large for a single session (1,100 trials), this number is insufficient for training deep learning models, which depend on both intra- and inter-subject variability to generalize well.

- **Datasets Heterogeneity:** The PhysioNet, AlexMI, and experimental recordings differed in electrode layouts, sampling rates, recording systems, and paradigms. Even though a shared preprocessing pipeline was applied, these domain shifts limited the utility of transfer learning, as models had to reconcile incompatible input distributions.

- **Reduced Spatial Resolution:** The use of only eight EEG channels to facilitate fast setup and real-world usability, restricted spatial information about cortical activity. MI decoding depends heavily on accurate localization of sensorimotor rhythms, especially over the midline and lateral motor areas, which may not be fully captured with such a sparse configuration.

5 CONCLUSIONS AND FUTURE WORKS

5.1 CONCLUSIONS

This Master's Thesis explored the design and evaluation of a DL-based BCI system for the binary classification of EEG signals corresponding to MI of both feet versus a resting state. The long-term objective of this work is to enable intuitive and responsive control of a lower-limb exoskeleton through non-invasive neural signals, offering an alternative communication channel for individuals with motor impairments. To address this challenge, three state-of-the-art convolutional neural network architectures: EEGNet, EEGInception, and EEGSym, were implemented and evaluated. A transfer learning strategy was adopted in which the models were pretrained using two publicly available datasets PhysioNet BCI2000 and AlexMI, and subsequently fine-tuned using a subject-specific dataset recorded with a reduced 8-channel EEG cap. The use of such a low-density setup aimed to enhance practical usability by reducing setup time, but also introduced challenges related to reduced spatial resolution.

Despite the use of modern architectures and a robust preprocessing pipeline, the results indicate that none of the models achieved satisfactory classification performance. Accuracy scores remained below 60%, and F1-scores did not exceed 0.55. While EEGNet achieved the best overall performance in terms of accuracy, precision, and recall, it also presented a high false negative rate for MI. EEGSym, in contrast, showed greater sensitivity to MI but suffered from high false positives during rest. EEGInception consistently underperformed across all metrics. These results highlight the difficulty of achieving both responsiveness and stability in real-time BCI applications using deep learning under realistic constraints. A key insight derived from this work is that data quality and consistency are far more limiting than model architecture. Even the most advanced neural networks are highly sensitive to mismatches in data distribution, task labels, recording setups, and signal noise. In this study, the scarcity of training data, label misalignment during pretraining, and differences across datasets such as electrode configuration, sampling rate, and experimental protocols, greatly limited the learning capacity of all models. Furthermore, the use of only eight EEG channels restricted the system's ability to capture the cortical topography associated with MI.

Nonetheless, this MSc thesis provides a solid foundation for future work by exposing the practical challenges of real-world BCI design and identifying critical areas for improvement. It demonstrates that while DL holds substantial promises for EEG decoding, its successful application in BCI systems depends on addressing several methodological and technical barriers.

5.2 FUTURE WORKS

Based on the findings and limitations identified throughout this project, several promising directions can be proposed to advance the effectiveness and applicability of EEG-based DL models for BCI-controlled lower-limb exoskeletons:

- **Expand the Dataset with More Participants and Trials:** One of the most urgent priorities is to collect data from a larger and more diverse pool of participants, under standardized recording protocols. This would allow models to learn inter-subject invariances and generalize better across individuals. Increasing the number of trials per class would also reduce overfitting and improve the robustness of subject-specific adaptation.

- **Align Pretraining and Target Tasks More Precisely:** Future work should use pretraining datasets that better reflect the same classification objective as the fine-tuning task. Datasets that explicitly label "rest" vs. "motor imagery of feet" should be prioritized to prevent semantic drift during training. If unavailable, it may be necessary to create new datasets with consistent labels and paradigms.

- **Introducing Data Augmentation Techniques:** To combat data scarcity and improve model generalization, data augmentation strategies could be explored. These include temporal

cropping, frequency shifting, additive noise, and synthetic signal generation using generative models or signal transformations. Augmentation can be applied both during pretraining and fine-tuning to increase dataset variability without requiring new acquisitions.

- **Improve Spatial Resolution with Optimal Electrode Layouts:** While usability considerations support low-density EEG, future studies might investigate hybrid configurations with 16–32 electrodes focused on the sensorimotor cortex. This would preserve spatial specificity without compromising portability.

- **Enhance Interpretability and Explainability:** To improve trust and facilitate clinical adoption, future work may also focus on developing interpretable DL models for EEG. Tools such as saliency maps, layer-wise relevance propagation, or attention mechanisms could help visualize which signal components the model relies on for decision-making.

In conclusion, this MSc Thesis provides both functional implementation and a critical examination of DL strategies in MI-based BCI systems. While results highlight current limitations, they also outline clear and feasible pathways toward more robust, adaptive, and user-friendly neurotechnological interfaces.

6 ETHICAL, ECONOMIC, SOCIETAL AND ENVIRONMENTAL ASPECTS

5.1 INTRODUCTION

The increasing demand for accessible and effective neurorehabilitation solutions has led to the development of BCI systems as a promising alternative to traditional therapy. This project addresses the design of a deep learning-based BCI for the classification of MI signals from EEG, aimed at enabling the intuitive and non-invasive control of lower-limb exoskeletons. Such systems can contribute significantly to improving the quality of life for individuals with motor impairments by restoring a degree of autonomy in movement and interaction. Beyond the technical scope, this work is situated within a broader context of societal, ethical, economic, and environmental challenges. From an ethical standpoint, direct interaction with neural data requires strict attention to user privacy, safety, and consent. Economically, the system seeks to reduce the costs of long-term therapy through home-based rehabilitation solutions but also faces barriers in terms of affordability and accessibility. Societally, the project contributes to the inclusion of people with disabilities, although its success depends on equitable access and careful consideration of user needs. Environmentally, the use of non-invasive, low-power, and reusable technologies aligns with the goal of minimizing the ecological footprint of emerging biomedical devices.

This chapter explores these four key dimensions: ethical, economic, societal, and environmental, and reflects on the implications of the system developed in this thesis, both as a research prototype and as a foundation for future assistive technologies.

5.2 DESCRIPTION OF RELEVANT IMPACTS RELATED TO THE PROJECT

During the development of the project, particular attention was given to identifying and assessing the broader impacts of implementing a BCI-controlled lower-limb exoskeleton system. This analysis focused on societal, economic, and environmental sustainability dimensions, as well as the stakeholders most directly affected by the deployment of such technologies.

From a societal perspective, the most significant impact identified is the potential to improve autonomy and quality of life for individuals with motor impairments, such as those recovering from stroke or suffering from spinal cord injury. By enabling intuitive control of assistive devices through non-invasive brain signals, the system supports greater independence in daily activities, contributing to social inclusion and dignity. However, successful implementation requires ongoing attention to usability, accessibility, and cognitive load, particularly for vulnerable populations. Key stakeholders in this context include patients, caregivers, healthcare providers, and rehabilitation specialists. On the economic side, the project has the potential to reduce the long-term costs of neurorehabilitation by allowing personalized, semi-autonomous home therapy. This could ease the burden on healthcare systems and reduce dependence on continuous clinical supervision. Nevertheless, the initial costs associated with BCI hardware, signal processing units, and robotic exoskeletons remain high. Therefore, early adoption may be limited to research institutions and specialized clinics. Manufacturers, healthcare institutions, insurance providers, and regulatory agencies were identified as primary economic stakeholders. In terms of environmental sustainability, the system demonstrates a relatively low ecological footprint due to its reliance on non-invasive, reusable EEG equipment and compact, energy-efficient embedded systems. Moreover, enabling at-home therapy reduces patient travel and associated emissions. That said, environmental impact may arise from the production and disposal of electronic components, highlighting the need for sustainable design practices. Environmental stakeholders include manufacturers, medical device regulators, and sustainability-focused research bodies.

The conclusions drawn from this impact assessment emphasize that the societal and economic benefits are potentially significant, provided the system is designed with inclusivity, scalability, and sustainability in mind. These considerations were carried forward into the system design and

discussed in later sections, with the aim of promoting not only technical innovation, but also responsible and ethical deployment of BCI technologies.

5.3 DETAILED ANALYSIS OF ONE OF THE PRINCIPAL IMPACTS

Among the various impacts identified during the project, the societal impact stands out as the most relevant, particularly in terms of the system's potential to improve functional independence and social inclusion for individuals with motor impairments. This section presents a more detailed analysis of this dimension, based on the system's intended use, the needs of the target population, and the practical conditions required for adoption. The core objective of the system is to enable users to interact with a lower-limb exoskeleton through MI-based brain signals, bypassing traditional control mechanisms and thereby offering a form of communication and interaction to those with severely reduced mobility. This capability is especially beneficial in the context of neurorehabilitation, where active participation and voluntary intention are key components of recovery. By facilitating movement through cognitive effort alone, the system offers the potential to reinforce neuroplasticity and support motor recovery, especially in early stages of rehabilitation.

To ensure a positive societal impact, several aspects must be addressed. First, the usability of the system must accommodate users with cognitive or motor limitations, meaning the interface must be intuitive, comfortable, and require minimal setup. The decision to use an 8-channel EEG cap in this project reflects this concern, balancing signal quality with practical constraints such as setup time and user comfort. Second, training protocols must be tailored to everyone, as the ability to perform MI tasks varies significantly among users. Third, and perhaps most importantly, accessibility and affordability must be considered from the early stages of development to avoid reinforcing inequalities in healthcare access. The principal stakeholders affected by this impact include patients, who are the direct beneficiaries; clinicians and rehabilitation professionals, who play a key role in deployment and monitoring; and caregivers and family members, who may experience reduced burden if the system enables greater user autonomy. Additionally, technology developers and healthcare institutions must work collaboratively to translate research prototypes into scalable, deployable solutions.

The analysis concludes that while the societal potential of BCI-based exoskeleton control systems is substantial, their true impact will depend on factors that extend beyond technical performance. A human-centered design approach, focused on usability, personalization, and ethical deployment, will be essential to ensure that such technologies are not only innovative, but also inclusive and socially beneficial.

5.4 CONCLUSIONS

From an integrated perspective, the project demonstrates a strong alignment with core sustainability principles, particularly in terms of ethical responsibility, social impact, economic feasibility, and environmental awareness. While the main objective was the development and evaluation of a DL-based BCI system for lower-limb exoskeleton control, sustainability considerations have played a significant role in shaping both the design decisions and the broader implications of the work.

From an ethical standpoint, the use of non-invasive EEG technology ensures that the system respects user autonomy, safety, and dignity, minimizing medical risk and preserving the privacy of neural data. The project’s adherence to informed consent protocols and human-subject research ethics further reinforces its ethical robustness. In terms of societal value, the system addresses a pressing need for accessible rehabilitation solutions and offers a path toward enhanced mobility and independence for individuals with motor impairments. The emphasis on ease of use, low hardware complexity, and user adaptability aligns with inclusive design principles and increases the likelihood of real-world adoption. This reflects a clear effort to generate social benefit and reduce inequality in access to advanced assistive technologies. From an economic perspective, while the

current implementation may still be limited by cost barriers, the project contributes to long-term affordability by exploring minimal EEG configurations and scalable architectures. These elements position the system as a viable candidate for future integration into cost-effective home-based rehabilitation programs, which could alleviate pressure on healthcare systems. Regarding environmental impact, the project promotes the use of reusable, efficient, and compact EEG and processing hardware, thus reducing the ecological footprint associated with frequent clinic rehabilitation. Moreover, enabling home therapy could indirectly lower transportation-related emissions, further reinforcing the project's sustainability value.

In conclusion, the deliberate incorporation of sustainability criteria has not only enhanced the relevance and responsibility of the project but also increased its real-world viability and potential for long-term societal benefit. Continued attention to these dimensions in future iterations through more inclusive design, scalable deployment, and green engineering practices will be essential to maximize the positive impact of BCI-based rehabilitation technologies.

7 FINANCIAL BUDGET

PERSONNEL COSTS (direct costs)	Hours	Hourly cost	Total
	650	10 €	**6.500 €**

MATERIAL RESROURCES COSTS (direct costs, DC)	Purchase price	Months of use	Depreciation (in years)	Total
Personal computer, including software	800,00 €	5	5	0,00 € (own use)
EEG Bitbrain 8ch	5.000 €	5	5	416,67 €
Exo-H3 Technaid	80.000,00 €	5	10	3.333,33 €
Other equipment (EEG accessories)				200,00 €

TOTAL COSTS OF MATERIAL RESOURCES	3.950,00 €

GENERAL COSTS (indirect costs, IC)	15%	on DC	592,50 €
INDUSTRIAL BENEFIT	6%	on DC+IC	271,05 €

CONSUMABLES

Printouts	0,00 €
Binding	0,00 €

SUBTOTAL BUDGET		11.313,25 €
VAT	21%	2.375,78 €

TOTAL BUDGET	13.689,03 €

8 BIBLIOGRAPHY

Alzubaidi, L., Zhang, J., Humaidi, A. J., Al-Dujaili, A., Duan, Y., Al-Shamma, O., Santamaría, J., Fadhel, M. A., Al-Amidie, M., & Farhan, L. (2021). Review of deep learning: concepts, CNN architectures, challenges, applications, future directions. *Journal of Big Data 2021 8:1*, *8*(1), 1–74. https://doi.org/10.1186/S40537-021-00444-8

Ang, K. K., & Guan, C. (2017). EEG-Based Strategies to Detect Motor Imagery for Control and Rehabilitation. *IEEE Transactions on Neural Systems and Rehabilitation Engineering*, *25*(4), 392–401. https://doi.org/10.1109/TNSRE.2016.2646763

Ávila-Tomás, J. F., Mayer-Pujadas, M. A., & Quesada-Varela, V. J. (2021). La inteligencia artificial y sus aplicaciones en medicina II: importancia actual y aplicaciones prácticas. *Atención Primaria*, *53*(1), 81–88. https://doi.org/10.1016/J.APRIM.2020.04.014

Baldwin, C. L., & Penaranda, B. N. (2012). Adaptive training using an artificial neural network and EEG metrics for within- and cross-task workload classification. *NeuroImage*, *59*(1), 48–56. https://doi.org/10.1016/J.NEUROIMAGE.2011.07.047

Barachant, A. (2012). Commande robuste d'un effecteur par une interface cerveau machine EEG asynchrone [Université de Grenoble]. In *Alexandre Barachant. Commande robuste d'un effecteur par une interface cerveau machine EEG asynchrone. Traitement du signal et de l'image [eess.SP]. Université de Grenoble, 2012. Français. ⟨NNT : 2012GRENT112⟩. ⟨tel-01196752⟩.* https://doi.org/10.34894/VQ1DJA

Belal, M., Alsheikh, N., Aljarah, A., & Hussain, I. (2024). Deep Learning Approaches for Enhanced Lower-Limb Exoskeleton Control: A Review. *IEEE Access*, *12*, 143883–143907. https://doi.org/10.1109/ACCESS.2024.3414175

Blankertz, B., Tomioka, R., Lemm, S., Kawanabe, M., & Müller, K.-R. (2008). Optimizing Spatial Filters for Robust EEG Single-Trial Analysis. *IEEE SIGNAL PROCESSING MAGAZINE*, *20*.

Branco, M. P., Pels, E. G. M., Sars, R. H., Aarnoutse, E. J., Ramsey, N. F., Vansteensel, M. J., & Nijboer, F. (2021). Brain-Computer Interfaces for Communication: Preferences of Individuals With Locked-in Syndrome. *Neurorehabilitation and Neural Repair*, *35*(3), 267–279. https://doi.org/10.1177/1545968321989331/SUPPL_FILE/SJ-PDF-1-NNR-10.1177_1545968321989331.PDF

Cantillo-Negrete, J., Carino-Escobar, R. I., Ortega-Robles, E., & Arias-Carrión, O. (2023). A comprehensive guide to BCI-based stroke neurorehabilitation interventions. *MethodsX*, *11*, 102452. https://doi.org/10.1016/J.MEX.2023.102452

Chaudhary, U., Birbaumer, N., & Ramos-Murguialday, A. (2016). Brain–computer interfaces for communication and rehabilitation. *Nature Reviews Neurology 2016 12:9*, *12*(9), 513–525. https://doi.org/10.1038/nrneurol.2016.113

Choi, R. Y., Coyner, A. S., Kalpathy-Cramer, J., Chiang, M. F., & Peter Campbell, J. (2020). Introduction to machine learning, neural networks, and deep learning. *Translational Vision Science and Technology*, *9*(2). https://doi.org/10.1167/TVST.9.2.14,

Chollet, F. (2017). Deep Learning with Python. In *Machine Learning* (Vol. 45, Issue 13). https://www.manning.com/books/deep-learning-with-python

Cohen, M. X. (2017). Where Does EEG Come From and What Does It Mean? *Trends in Neurosciences*, *40*(4), 208–218. https://doi.org/10.1016/J.TINS.2017.02.004/ATTACHMENT/C2F85FB8-53B0-47EA-A673-A4865BC81687/MMC1.PDF

Coogan, C. G., & He, B. (2018). Brain-Computer Interface Control in a Virtual Reality Environment and Applications for the Internet of Things. *IEEE Access*, *6*, 10840–10849. https://doi.org/10.1109/ACCESS.2018.2809453

de Miguel-Fernández, J., Lobo-Prat, J., Prinsen, E., Font-Llagunes, J. M., & Marchal-Crespo, L. (2023). Control strategies used in lower limb exoskeletons for gait rehabilitation after brain injury: a systematic review and analysis of clinical effectiveness. *Journal of NeuroEngineering and Rehabilitation*, *20*(1). https://doi.org/10.1186/S12984-023-01144-5,

Decety, J. (1996). The neurophysiological basis of motor imagery. *Behavioural Brain Research*, *77*(1–2), 45–52. https://doi.org/10.1016/0166-4328(95)00225-1

Faller, J., Scherer, R., Costa, U., Opisso, E., Medina, J., & Müller-Putz, G. R. (2014). A Co-Adaptive Brain-Computer Interface for End Users with Severe Motor Impairment. *PLOS ONE*, *9*(7), e101168. https://doi.org/10.1371/JOURNAL.PONE.0101168

Gerloff, C., Richard, J., Hadley, J., Schulman, A. E., Honda, M., & Hallett, M. (1998). Functional coupling and regional activation of human cortical motor areas during simple, internally paced and externally paced finger movements. *Brain*, *121*(8), 1513–1531. https://doi.org/10.1093/BRAIN/121.8.1513

Goldberger, A. L., Amaral, L. A., Glass, L., Hausdorff, J. M., Ivanov, P. C., Mark, R. G., Mietus, J. E., Moody, G. B., Peng, C. K., & Stanley, H. E. (2000). PhysioBank, PhysioToolkit, and PhysioNet: components of a new research resource for complex physiologic signals. *Circulation*, *101*(23). https://doi.org/10.1161/01.CIR.101.23.E215/ASSET/9716B30D-2E4D-4D06-8F9E-A21157DFE97C/ASSETS/GRAPHIC/HC2304183003.JPEG

Gomez-Pilar, J., Corralejo, R., Nicolas-Alonso, L. F., Alvarez, D., & Hornero, R. (2014). Assessment of neurofeedback training by means of motor imagery based-BCI for cognitive rehabilitation. *2014 36th Annual International Conference of the IEEE Engineering in Medicine and Biology Society*, 3630–3633. https://doi.org/10.1109/EMBC.2014.6944409

Iftikhar, M., Khan, S. A., & Hassan, A. (2018). A Survey of Deep Learning and Traditional Approaches for EEG Signal Processing and Classification. *2018 IEEE 9th Annual Information Technology, Electronics and Mobile Communication Conference, IEMCON 2018*, 395–400. https://doi.org/10.1109/IEMCON.2018.8614893

Jafari, Z., Kolb, B. E., & Mohajerani, M. H. (2020). Neural oscillations and brain stimulation in Alzheimer's disease. *Progress in Neurobiology*, *194*. https://doi.org/10.1016/j.pneurobio.2020.101878

Jamil, N., Belkacem, A. N., Ouhbi, S., & Guger, C. (2021). Cognitive and affective brain-computer interfaces for improving learning strategies and enhancing student capabilities: A systematic literature review. *IEEE Access*, *9*, 134122–134147. https://doi.org/10.1109/ACCESS.2021.3115263

Jiang, X., Bian, G. Bin, & Tian, Z. (2019). Removal of Artifacts from EEG Signals: A Review. *Sensors 2019, Vol. 19, Page 987*, *19*(5), 987. https://doi.org/10.3390/S19050987

Kamath, C. N., Bukhari, S. S., & Dengel, A. (2018). Comparative study between traditional machine learning and deep learning approaches for text classification. *Association for Computing Machinery*. https://doi.org/10.1145/3209280.3209526;TOPIC:TOPIC:CONFERENCE-COLLECTIONS>DOCENG;JOURNAL:JOURNAL:ACMCONFERENCES;PAGEGROUP:STRING:PUBLICATION

Kawala-Sterniuk, A., Browarska, N., Al-Bakri, A., Pelc, M., Zygarlicki, J., Sidikova, M., Martinek, R., & Gorzelanczyk, E. J. (2021). Summary of over Fifty Years with Brain-Computer Interfaces-A Review. *Brain Sciences*, *11*(1), 43. https://doi.org/10.3390/brainsci

Keirn, Z. A., & Aunon, J. I. (1990). A New Mode of Communication Between Man and his Surroundings. *IEEE Transactions on Biomedical Engineering*, *37*(12), 1209–1214. https://doi.org/10.1109/10.64464

Kevric, J., & Subasi, A. (2017). Comparison of signal decomposition methods in classification of EEG signals for motor-imagery BCI system. *Biomedical Signal Processing and Control*, *31*, 398–406. https://doi.org/10.1016/J.BSPC.2016.09.007

Kübler, A., Nijboer, F., Mellinger, J., Vaughan, T. M., Pawelzik, H., Schalk, G., McFarland, D. J., Birbaumer, N., & Wolpaw, J. R. (2005). Patients with ALS can use sensorimotor rhythms to operate a brain-computer interface. *Neurology*, *64*(10), 1775–1777. https://doi.org/10.1212/01.WNL.0000158616.43002.6D

Ladda, A. M., Lebon, F., & Lotze, M. (2021). Using motor imagery practice for improving motor performance – A review. *Brain and Cognition*, *150*, 105705. https://doi.org/10.1016/J.BANDC.2021.105705

Lawhern, V. J., Solon, A. J., Waytowich, N. R., Gordon, S. M., Hung, C. P., & Lance, B. J. (2018). EEGNet: a compact convolutional neural network for EEG-based brain–computer interfaces. *Journal of Neural Engineering*, *15*(5), 056013. https://doi.org/10.1088/1741-2552/AACE8C

Lebedev, M. A., & Nicolelis, M. A. L. (2006). Brain–machine interfaces: past, present and future. *Trends in Neurosciences*, *29*(9), 536–546. https://doi.org/10.1016/J.TINS.2006.07.004

Lee, T. S., Goh, S. J. A., Quek, S. Y., Phillips, R., Guan, C., Cheung, Y. B., Feng, L., Teng, S. S. W., Wang, C. C., Chin, Z. Y., Zhang, H., Ng, T. P., Lee, J., Keefe, R., & Krishnan, K. R. R. (2013). A Brain-Computer Interface Based Cognitive Training System for Healthy Elderly: A Randomized Control Pilot Study for Usability and Preliminary Efficacy. *PLOS ONE*, *8*(11), e79419. https://doi.org/10.1371/JOURNAL.PONE.0079419

Liu, S., Zhang, J., Wang, A., -, al, Wu, H., Xie, Q., Yu, Z., Liu, X., Lv, L., Shen, Y., Craik, A., He, Y., & Contreras-Vidal, J. L. (2019). Deep learning for electroencephalogram (EEG) classification tasks: a review. *Journal of Neural Engineering*, *16*(3), 031001. https://doi.org/10.1088/1741-2552/AB0AB5

Lotte, F., Congedo, M., Lécuyer, A., Lamarche, F., & Arnaldi, B. (2007). A review of classification algorithms for EEG-based brain–computer interfaces. *Journal of Neural Engineering*, *4*(2), R1. https://doi.org/10.1088/1741-2560/4/2/R01

Lotte, F., Larrue, F., & Mühl, C. (2013). Flaws in current human training protocols for spontaneous Brain-Computer interfaces: Lessons learned from instructional design. *Frontiers in Human Neuroscience*, *7*(SEP), 50380. https://doi.org/10.3389/FNHUM.2013.00568/BIBTEX

Michel, C. M., & Brunet, D. (2019). EEG source imaging: A practical review of the analysis steps. *Frontiers in Neurology*, *10*(APR), 10–325. https://doi.org/10.3389/FNEUR.2019.00325,

Milekovic, T., Sarma, A. A., Bacher, D., Simeral, J. D., Saab, J., Pandarinath, C., Sorice, B. L., Blabe, C., Oakley, E. M., Tringale, K. R., Eskandar, E., Cash, S. S., Henderson, J. M., Shenoy, K. V., Donoghue, J. P., & Hochberg, L. R. (2018). Stable long-term BCI-enabled communication in ALS and locked-in syndrome using LFP signals. *Journal of Neurophysiology*, *120*(1), 343–360. https://doi.org/10.1152/JN.00493.2017/SUPPL_FILE/MOVIE

Neuper, C., Scherer, R., Wriessnegger, S., & Pfurtscheller, G. (2009). Motor imagery and action observation: Modulation of sensorimotor brain rhythms during mental control of a brain–computer interface. *Clinical Neurophysiology*, *120*(2), 239–247. https://doi.org/10.1016/J.CLINPH.2008.11.015

Nicolas-Alonso, L. F., Corralejo, R., Gomez-Pilar, J., Álvarez, D., & Hornero, R. (2015). Adaptive semi-supervised classification to reduce intersession non-stationarity in multiclass motor imagery-based brain–computer interfaces. *Neurocomputing*, *159*(1), 186–196. https://doi.org/10.1016/J.NEUCOM.2015.02.005

Nunez, P. L., & Srinivasan, R. (2006). Electric Fields of the Brain: The neurophysics of EEG. *Oxford Academic*, 1–611. https://doi.org/10.1093/ACPROF:OSO/9780195050387.001.0001

Onishi, A., & Natsume, K. (2014). Overlapped Partitioning for Ensemble Classifiers of P300-Based Brain-Computer Interfaces. *PLOS ONE*, *9*(4), e93045. https://doi.org/10.1371/JOURNAL.PONE.0093045

Padfield, N., Zabalza, J., Zhao, H., Masero, V., & Ren, J. (2019). EEG-Based Brain-Computer Interfaces Using Motor-Imagery: Techniques and Challenges. *Sensors 2019, Vol. 19, Page 1423*, *19*(6), 1423. https://doi.org/10.3390/S19061423

Perez-Velasco, S., Santamaria-Vazquez, E., Martinez-Cagigal, V., Marcos-Martinez, D., & Hornero, R. (2022). EEGSym: Overcoming Inter-Subject Variability in Motor Imagery Based BCIs With Deep Learning. *IEEE Transactions on Neural Systems and Rehabilitation Engineering*, *30*, 1766–1775. https://doi.org/10.1109/TNSRE.2022.3186442

Pfurtscheller, G., Brunner, C., Schlögl, A., & Lopes da Silva, F. H. (2006). Mu rhythm (de)synchronization and EEG single-trial classification of different motor imagery tasks. *NeuroImage*, *31*(1), 153–159. https://doi.org/10.1016/J.NEUROIMAGE.2005.12.003

Pfurtscheller, G., Guger, C., Müller, G., Krausz, G., & Neuper, C. (2000). Brain oscillations control hand orthosis in a tetraplegic. *Neuroscience Letters*, *292*(3), 211–214. https://doi.org/10.1016/S0304-3940(00)01471-3

Pfurtscheller, G., & Neuper, C. (2001). Motor imagery direct communication. *Proceedings of the IEEE*, *89*(7), 1123–1134. https://doi.org/10.1109/5.939829

Purves, D., Augustine, G. J., Fitzpatrick, D., Katz, L. C., LaMantia, A.-S., McNamara, J. O., & Williams, S. M. (2001). The Primary Motor Cortex: Upper Motor Neurons That Initiate Complex Voluntary Movements. In *Neuroscience. 2nd edition.* (2nd ed.). Sinauer Associates. https://www.ncbi.nlm.nih.gov/books/NBK10962/

Ramadan, R. A., & Vasilakos, A. V. (2017). Brain computer interface: control signals review. *Neurocomputing*, *223*, 26–44. https://doi.org/10.1016/J.NEUCOM.2016.10.024

Ramos-Murguialday, A., Broetz, D., Rea, M., Läer, L., Yilmaz, Ö., Brasil, F. L., Liberati, G., Curado, M. R., Garcia-Cossio, E., Vyziotis, A., Cho, W., Agostini, M., Soares, E., Soekadar, S., Caria, A., Cohen, L. G., & Birbaumer, N. (2013). Brain–machine interface in chronic stroke rehabilitation: A controlled study. *Annals of Neurology*, *74*(1), 100–108. https://doi.org/10.1002/ANA.23879

Ridderinkhof, K. R., & Brass, M. (2015). How Kinesthetic Motor Imagery works: A predictive-processing theory of visualization in sports and motor expertise. *Journal of Physiology-Paris*, *109*(1–3), 53–63. https://doi.org/10.1016/J.JPHYSPARIS.2015.02.003

Ruiz-Gómez, S. J., Hornero, R., Poza, J., Maturana-Candelas, A., Pinto, N., & Gómez, C. (2019). Computational modeling of the effects of EEG volume conduction on functional connectivity metrics. Application to Alzheimer's disease continuum. *Journal of Neural Engineering*, *16*(6). https://doi.org/10.1088/1741-2552/AB4024,

Saha, S., & Baumert, M. (2020). Intra- and Inter-subject Variability in EEG-Based Sensorimotor Brain Computer Interface: A Review. *Frontiers in Computational Neuroscience*, *13*, 506286. https://doi.org/10.3389/FNCOM.2019.00087/BIBTEX

Sanei, S., & Chambers, J. A. (2013). EEG Signal Processing. In *EEG Signal Processing*. John Wiley and Sons. https://doi.org/10.1002/9780470511923

Santamaría-Vázquez, E., Martínez-Cagigal, V., Marcos-Martínez, D., Rodríguez-González, V., Pérez-Velasco, S., Moreno-Calderón, S., & Hornero, R. (2023). MEDUSA©: A novel Python-based software ecosystem to accelerate brain-computer interface and cognitive neuroscience research. *Computer Methods and Programs in Biomedicine*, *230*, 107357. https://doi.org/10.1016/J.CMPB.2023.107357

Santamaría-Vázquez, E., Martínez-Cagigal, V., Vaquerizo-Villar, F., Hornero, R., & Member, S. (2020). EEG-Inception: A Novel Deep Convolutional Neural Network for Assistive ERP-Based

Brain-Computer Interfaces. *IEEE* , *28*(12), 2773–2782. https://doi.org/10.1109/TNSRE.2020.3048106

Sazgar, M., & Young, M. G. (2019). EEG Artifacts. In *Absolute Epilepsy and EEG Rotation Review*. Springer, Cham. https://doi.org/10.1007/978-3-030-03511-2_8

Schalk, G., McFarland, D. J., Hinterberger, T., Birbaumer, N., & Wolpaw, J. R. (2004). BCI2000: A general-purpose brain-computer interface (BCI) system. *IEEE Transactions on Biomedical Engineering*, *51*(6), 1034–1043. https://doi.org/10.1109/TBME.2004.827072

Schalk, Gerwin, J McFarland, D., Hinterberger, T., Birbaumer, N., & Wolpaw, J. R. (2022). EEG Motor Movement/Imagery Dataset . In *PhysioNet*. https://doi.org/https://doi.org/10.13026/C28G6P

Schirrmeister, R. T., Springenberg, J. T., Fiederer, L. D. J., Glasstetter, M., Eggensperger, K., Tangermann, M., Hutter, F., Burgard, W., & Ball, T. (2017). Deep learning with convolutional neural networks for EEG decoding and visualization. *Human Brain Mapping*, *38*(11), 5391–5420. https://doi.org/10.1002/HBM.23730

Sensslite, B. (2025, June 21). *SENNSLITE®*. Bitbrain.Com. https://www.bitbrain.com/es/productos-neurotecnologia/software/sennslite

Shih, J. J., Krusienski, D. J., & Wolpaw, J. R. (2012). Brain-Computer Interfaces in Medicine. *Mayo Clinic Proceedings*, *87*(3), 279. https://doi.org/10.1016/J.MAYOCP.2011.12.008

Sibilano, E., Suglia, V., Brunetti, A., Buongiorno, D., Caporusso, N., Guger, C., & Bevilacqua, V. (2024). Brain–Computer Interfaces. *Neuromethods*, *206*, 203–240. https://doi.org/10.1007/978-1-0716-3545-2_10

Song, J., Davey, C., Poulsen, C., Luu, P., Turovets, S., Anderson, E., Li, K., & Tucker, D. (2015). EEG source localization: Sensor density and head surface coverage. *Journal of Neuroscience Methods*, *256*, 9–21. https://doi.org/10.1016/j.jneumeth.2015.08.015

Supapitanon, K., Patathong, T., Akkawutvanich, C., Srisuchinnawong, A., Ketrungsri, W., Manoonpong, P., Woratanarat, P., & Angsanuntsukh, C. (2025). Comprehensive multi-metric analysis of user experience and performance in adaptive and non-adaptive lower-limb exoskeletons. *PLOS ONE*, *20*(1), e0313593. https://doi.org/10.1371/JOURNAL.PONE.0313593

Technaid. (2025). *Exo-H3 Technaid*. https://www.technaid.com/es/productos/robotic-exoskeleton-exo-h3/

Versatile Water-based EEG cap, B. (2025, June 21). *Versatile Water-based EEG cap*. Bitbrain.Com. https://www.bitbrain.com/neurotechnology-products/water-based-eeg/versatile-eeg

Vidal, J. J. (1973). Toward Direct Brain-Computer Communication. *Annual Reviews of Biophysics*, *2*, 157–180. https://doi.org/10.1146/annurev.bb.02.060173.001105

Wolpaw, J. R., & McFarland, D. J. (2004). Control of a two-dimensional movement signal by a noninvasive brain-computer interface in humans. *Proceedings of the National Academy of Sciences of the United States of America*, *101*(51), 17849–17854. https://doi.org/10.1073/PNAS.0403504101/SUPPL_FILE/03504MOVIE1.MOV

Wolpaw, J. R., McFarland, D. J., Neat, G. W., & Forneris, C. A. (1991). An EEG-based brain-computer interface for cursor control. *Electroencephalography and Clinical Neurophysiology*, *78*(3), 252–259. https://doi.org/10.1016/0013-4694(91)90040-B

Wolpaw, J. R., & Wolpaw, E. W. (2012). Brain–Computer Interfaces: Principles and Practice. *Oxford Academic*, 1–424. https://doi.org/10.1093/ACPROF:OSO/9780195388855.001.0001

Yadav, D., Yadav, S., & Veer, K. (2020). A comprehensive assessment of Brain Computer Interfaces: Recent trends and challenges. *Journal of Neuroscience Methods*, *346*, 108918. https://doi.org/10.1016/J.JNEUMETH.2020.108918

Yang, Y. J., Jeon, E. J., Kim, J. S., & Chung, C. K. (2021). Characterization of kinesthetic motor imagery compared with visual motor imageries. *Scientific Reports*, *11*(1), 1–11.

https://doi.org/10.1038/S41598-021-82241-0;SUBJMETA=116,2629,378,631;KWRD=COMPUTATIONAL+NEUROSCIENCE,SENSORIMOTOR+PROCESSING

Yu, Q. H., Fu, A. S. N., Kho, A., Li, J., Sun, X. H., & Chan, C. C. H. (2016). Imagery perspective among young athletes: Differentiation between external and internal visual imagery. *Journal of Sport and Health Science*, *5*(2), 211–218. https://doi.org/10.1016/J.JSHS.2014.12.008

Yuan, H., & He, B. (2014). Brain-computer interfaces using sensorimotor rhythms: Current state and future perspectives. *IEEE Transactions on Biomedical Engineering*, *61*(5), 1425–1435. https://doi.org/10.1109/TBME.2014.2312397

Zich, C., Debener, S., Kranczioch, C., Bleichner, M. G., Gutberlet, I., & De Vos, M. (2015). Real-time EEG feedback during simultaneous EEG–fMRI identifies the cortical signature of motor imagery. *NeuroImage*, *114*, 438–447. https://doi.org/10.1016/J.NEUROIMAGE.2015.04.020

Zippo, A. G. (2011, April). Neuronal Ensemble Modeling and Analysis with Variable Order Markov Models Contents. *Phd Thesis*.